

AD-A119 879 NAVAL POSTGRADUATE SCHOOL MONTEREY CA F/G 11/6
AN INVESTIGATION INTO THE TWO-WAY SHAPE MEMORY TRAINABILITY OF --ETC(U)
JUN 82 R O SPONHOLZ

NAVAL POSTGRADUATE SCHOOL MONTEREY CA F/O 11/6:
AN INVESTIGATION INTO THE TWO-WAY SHAPE MEMORY TRAINABILITY OF --ETC(U)
JUN 82 R O SPONHOLZ

F/O 11/6.
OF --ETC(U)

NL

1000

END
DATE
FILMED
11 82
DTIC

AD A119579

NAVAL POSTGRADUATE SCHOOL
Monterey, California



DTIC
ELECTE
SEP 27 1982
S F D

THESIS

AN INVESTIGATION INTO THE TWO-WAY SHAPE
MEMORY TRAINABILITY OF POLYCRYSTALLINE
Cu-Zn-Al ALLOYS

by

Richard O. Sponholz

June 1982

Thesis Advisor:

A. J. Perkins

Approved for public release; distribution unlimited.

DTIC FILE COPY

82 09 27 030

SECURITY CLASSIFICATION OF THIS PAGE (When Data Entered)

REPORT DOCUMENTATION PAGE		READ INSTRUCTIONS BEFORE COMPLETING FORM
1. REPORT NUMBER	2. GOVT ACCESSION NO.	3. RECIPIENT'S CATALOG NUMBER
	AD-A119579	
4. TITLE (and Subtitle)		5. TYPE OF REPORT & PERIOD COVERED
An Investigation into the Two-Way Shape Memory Trainability of Polycrystalline Cu-Zn-Al Alloys		Master's Thesis; June 1982
7. AUTHOR(s)		6. PERFORMING ORG. REPORT NUMBER
Richard O. Sponholz		
9. PERFORMING ORGANIZATION NAME AND ADDRESS		8. CONTRACT OR GRANT NUMBER(s)
Naval Postgraduate School Monterey, California 93940		
11. CONTROLLING OFFICE NAME AND ADDRESS		10. PROGRAM ELEMENT, PROJECT, TASK AREA & WORK UNIT NUMBERS
Naval Postgraduate School Monterey, California 93940		
14. MONITORING AGENCY NAME & ADDRESS (if different from Controlling Office)		12. REPORT DATE
		June 1982
		13. NUMBER OF PAGES
		80
		15. SECURITY CLASS. (of this report)
		Unclassified
		15a. DECLASSIFICATION/DOWNGRADING SCHEDULE
16. DISTRIBUTION STATEMENT (of this Report)		
Approved for public release; distribution unlimited.		
17. DISTRIBUTION STATEMENT (of the abstract entered in Block 20, if different from Report)		
18. SUPPLEMENTARY NOTES		
19. KEY WORDS (Continue on reverse side if necessary and identify by block number)		
Martensite Shape Memory		
20. ABSTRACT (Continue on reverse side if necessary and identify by block number)		
<p>→ The ability of polycrystalline Cu-Zn-Al alloys to demonstrate increasing percentage two-way shape memory (TWSM) displacements with "training" is investigated. Results indicate a definite relationship between increased cycling and increased TWSM ability. The empirical training cycle curve parameters are presented and shown to change with cycling. Most parameters</p>		

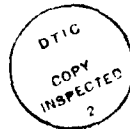
DD FORM 1473

1 JAN 73

EDITION OF 1 NOV 65 IS OBSOLETE
S/N 0102-014-6001

SECURITY CLASSIFICATION OF THIS PAGE (When Data Entered)

show a decreasing trend. Transmission electron microscopy of trained alloys is conducted in an effort to mechanistically explain TWSM training.



Accession For	
NTIS GRA&I	<input checked="" type="checkbox"/>
DTIC TAB	<input type="checkbox"/>
Unannounced	<input type="checkbox"/>
Justification	
By	
Distribution/	
Availability Codes	
Avail and/or	
Dist	Special
A	

Approved for public release; distribution unlimited.

An Investigation into the Two-Way Shape
Memory Trainability of Polycrystalline Cu-Zn-Al Alloys

by

Richard O. Sponholz
Lieutenant Commander, United States Navy
B.A., Queens College of the City University of New York,
1970

Submitted in partial fulfillment of the
requirements for the degree of

MASTER OF SCIENCE IN MECHANICAL ENGINEERING

from the

NAVAL POSTGRADUATE SCHOOL
June 1982

Author:

Richard O. Sponholz

Approved by:

Jeff Perkins

Thesis Advisor

Conrad D. Challenor

Second Reader

J. J. Marto

Chairman, Department of Mechanical Engineering

William M.oller

Dean of Science and Engineering

ABSTRACT

The ability of polycrystalline Cu-Zn-Al alloys to demonstrate increasing percentage two-way shape memory (TWSM) displacements with "training" is investigated. Results indicate a definite relationship between increased cycling and increased TWSM ability. The empirical training cycle curve parameters are presented and shown to change with cycling. Most parameters show a decreasing trend. Transmission electron microscopy of trained alloys is conducted in an effort to mechanistically explain TWSM training.

TABLE OF CONTENTS

I.	INTRODUCTION-----	11
II.	EXPERIMENTAL PROCEDURE-----	16
	A. ALLOY PREPARATION-----	16
	B. TRANSFORMATION TEMPERATURE DETERMINATION-----	16
	C. ALLOY TRAINING APPARATUS AND PROCEDURE-----	17
	D. DIFFERENTIAL SCANNING CALORIMETER RETESTING----	20
	E. TRANSMISSION ELECTRON MICROSCOPY-----	20
III.	RESULTS AND DISCUSSION-----	22
	A. DESCRIPTION OF THE TRAINING ROUTINE-----	22
	B. TRENDS IN TRAINING CYCLE PARAMETERS AS A FUNCTION OF THE NUMBER OF CYCLES-----	25
	1. Induced Displacement-----	26
	2. Elongation due to Thermoelastic Martensitic Transformation under Stress-----	31
	3. Total Elongation-----	33
	4. Peak Stress at Fixed Temperature-----	33
	5. Training Cycle Comparisons-----	39
	C. TWSM TRAINABILITY RESULTS-----	41
	D. DIFFERENTIAL SCANNING CALORIMETER DATA-----	46
	E. MECHANISMS OF TWSM-----	48
IV.	TRANSMISSION ELECTRON MICROSCOPY-----	51
V.	CONCLUSIONS-----	76
	LIST OF REFERENCES-----	78
	INITIAL DISTRIBUTION LIST-----	80

LIST OF TABLES

I.	Amount of Plastic Deformation (Δ_p) Retained in the Specimens after the First Training Cycle (in mils)-	24
II.	Induced Displacement (Δ_i) in mils-----	27
III.	Thermoelastic Martensitic Displacement (Δ_m) in mils-----	32
IV.	Peak Stress at Fixed Temperature-----	34
V.	Training Cycle Parameters - Typical Beginning and Ending Values-----	40
VI.	TWSM Performance-----	42
VII.	Differential Scanning Calorimeter Data-----	47

LIST OF FIGURES

1.	Schematic illustration of training routines used to obtain two-way shape memory (TWSM)-----	14
2.	Experimental Apparatus-----	19
3.	Grip Assembly and Sensor Arrangement-----	19
4A.	Typical Instron Chart Recording-----	23
4B.	Typical Displacement Chart Recording-----	23
5.	Induced Displacement (Δ_i) vs. Cycles. Specimen D-6 (20 training cycles)-----	28
6.	Induced Displacement (Δ_i) vs. Cycles. Specimen D-9 (20 training cycles)-----	29
7.	Induced Displacement (Δ_i) vs. Cycles. Specimen D-7 (30 training cycles)-----	30
8.	Peak Stress vs. Cycles. Specimen D-3 (10 training cycles)-----	36
9.	Peak Stress vs. Cycles. Specimen D-6 (20 training cycles)-----	37
10.	Peak Stress vs. Cycles. Specimen D-9 (20 training cycles)-----	38
11.	TWSM Trainability Results Composite-----	44
12.	TWSM Trainability Results Alloys D-7 (30 training cycles)-----	45
13.	Specimen D-11 (untrained). 23,500X-----	56
14.	Specimen D-10 (3 training cycles). Individual lines are dislocations. 39,000X-----	57
15.	Specimen D-10 (3 training cycles). Light and dark parallel regions are evidenced along with some straight features between uppermost parallel regions. 26,500X-----	58

16.	Specimen D-10 (3 training cycles). Same area as Figure 15 at 53,000X-----	59
17.	Specimen D-10 (3 training cycles). 79,500X-----	60
18.	Specimen D-5 (5 training cycles). Regions similar to those of specimen D-10 are shown. 26,500X-----	61
19.	Specimen D-5 (5 training cycles). Same area as Figure 18. 39,000X-----	62
20.	Specimen D-5 (5 training cycles). Preferential polishing has outlined areas where martensite plates existed. There are linear features, possibly dislocations on the left part of the photo micrograph. 39,000X-----	63
21.	Specimen D-4 (15 training cycles). Regions of former martensite plates are shown. A parallel array of dislocations is in the background. Parallel "vestigial" markings under lower plate region is shown. 26,500X-----	64
22.	Specimen D-4 (15 training cycles). Same region as Figure 21. 53,000X-----	65
23.	Specimen D-4 (15 training cycles). Same region as Figure 21. 79,500X-----	66
24.	Specimen D-4 (15 training cycles). Area between parallel markings. Dislocations are evident. Two parallel retained martensite plates appear in lower left. 26,500X-----	67
25.	Specimen D-6 (20 training cycles). Parallel bands similar to specimen D-10 (3 training cycles) are shown. 26,500X-----	68
26.	Specimen D-6 (20 training cycles). Same region as Figure 25 at 53,000X-----	69
27.	Specimen D-7 (30 training cycles). Retained martensite plate with heavily dislocated area surrounding them. 26,500X-----	70
28.	Specimen D-7 (30 training cycles). Martensite plate arrangement with debris adjoining plate area. 39,000X-----	71
29.	Specimen D-7 (30 training cycles). 79,500X-----	72

- 30. Diffraction pattern of area shown in Figure 29----- 73
- 31. Specimen D-7 (30 training cycles). Dislocation
tangles. 53,000X----- 74
- 32. Specimen D-7 (30 training cycles). Same area as
Figure 31 at 120,000X. Individual dislocations
can be seen.----- 75

ACKNOWLEDGMENT

Impetus for this investigation was provided by the sponsorship of the National Science Foundation research program: "Martensitic Transformations in Shape Memory Alloys."

Thanks are due to Professor Jeff Perkins for initial program formulation and continued guidance, and Tom Biogg for technical assistance. I would also like to thank Professor Michael Edwards, who first introduced me to the field of Materials Science, and who provided both motivation and expert instruction. Finally, I want to thank my wife, Pam and children, Luke and Alicia who have borne the costs of this research as surely as I.

I. INTRODUCTION

During the past decade, considerable study has been given to a number of alloys which exhibit so-called shape memory (SM). These alloys can undergo large amounts of strain and then upon temperature increase, or unloading, revert to their original shape without undergoing plastic deformation. Shape memory has been demonstrated in a number of alloys, both binary (Ni-Ti, AuCd) and tertiary (Cu-Al-Ni). The subject alloy of this investigation is Cu-Zn-Al.

The literature of shape memory is rife with special terminology. The terms used in this work will generally be those delineated by Perkins [Ref. 1].

A short summary of terms is in order:

a. Shape Memory (SM) - is a general term which refers to various thermoelastic behaviors where there is a reversal of apparent plastic strain.

b. Shape Memory Effect (SME) - a specimen which has been deformed maintains that deformation when applied stress is removed, but recovers its original shape when heated.

c. Stress Induced Martensite (SIM) - a specimen is deformed while in the parent phase (at a temperature $> M_s$ temperature), producing martensite.

d. Pseudoelastic Effect - the specimen recovers a proportion of the induced strain immediately on unloading.

e. Two-Way Shape Memory (TWSM) - a specimen changes shape in two directions as a function of temperature (heating and cooling). In effect, the alloy remembers both high and low temperature shapes. TWSM can be achieved by subjecting a specimen to a number of SME cycles, SIM cycles or, as in this work, a series of combined SIM-SME cycles.

The essence of shape memory depends upon the alloy's ability to undergo a thermoelastic or pseudoelastic martensitic transformation. A thermoelastic martensitic transformation is realized if martensite forms and grows continuously as the temperature is lowered, and shrinks and vanishes continuously along the same path as temperature is raised. A pseudoelastic transformation is the mechanical analogue to thermoelastic transformation. In this case the martensite grows continuously as stress is applied and is reversed as stress is decreased [Ref. 2]. In effect, cooling or the application of stress promotes the martensitic transformation while heating or unstressing reverses it [Ref. 1]. This principle will be utilized to provide a training routine for two-way shape memory.

The Cu-Zn-Al alloy exists in the parent phase as a BCC crystal structure. When this parent phase is subsequently cooled or stressed, mutually accommodating martensite plates grow. The reason for the reversibility of this martensite is that, unlike ferrous alloys, there are low elastic strains

associated with this transformation. The elastic strain limit of the parent phase is not exceeded (provided applied strain is within limits) and thus no plastic deformation takes place [Ref. 1]. When an alloy in the martensitic condition is stressed, or in the case of stress induced martensite subsequently cooled, the martensite plates grow, shrink and adjust themselves with neighboring plates. The result is the plates align themselves in the most favorable manner under the application of stress and once again, provided applied strain is within limits, no plastic deformation takes place.

As previously noted, two-way shape memory can be generated by subjecting a specimen to a series of SIM/SME cycles. Perkins has suggested such a training cycle, Figure 1, taken from Ref. 1, while Delaey utilized a similar training routine while cinefilming microstructure changes as a function of training cycles [Ref. 3].

The purpose of this work was to investigate the effects of subjecting specimens to training routines. Of particular interest was whether or not the experimental data would confirm the general shape of the training cycle as depicted schematically in Figure 1. That is, what values of stress and displacement are exhibited as the specimen is subjected to a single training cycle and in what manner do these values change as a function of the number of cycles to which the specimen is subjected. More importantly, this work is concerned with the ability of specimens to improve their two-way

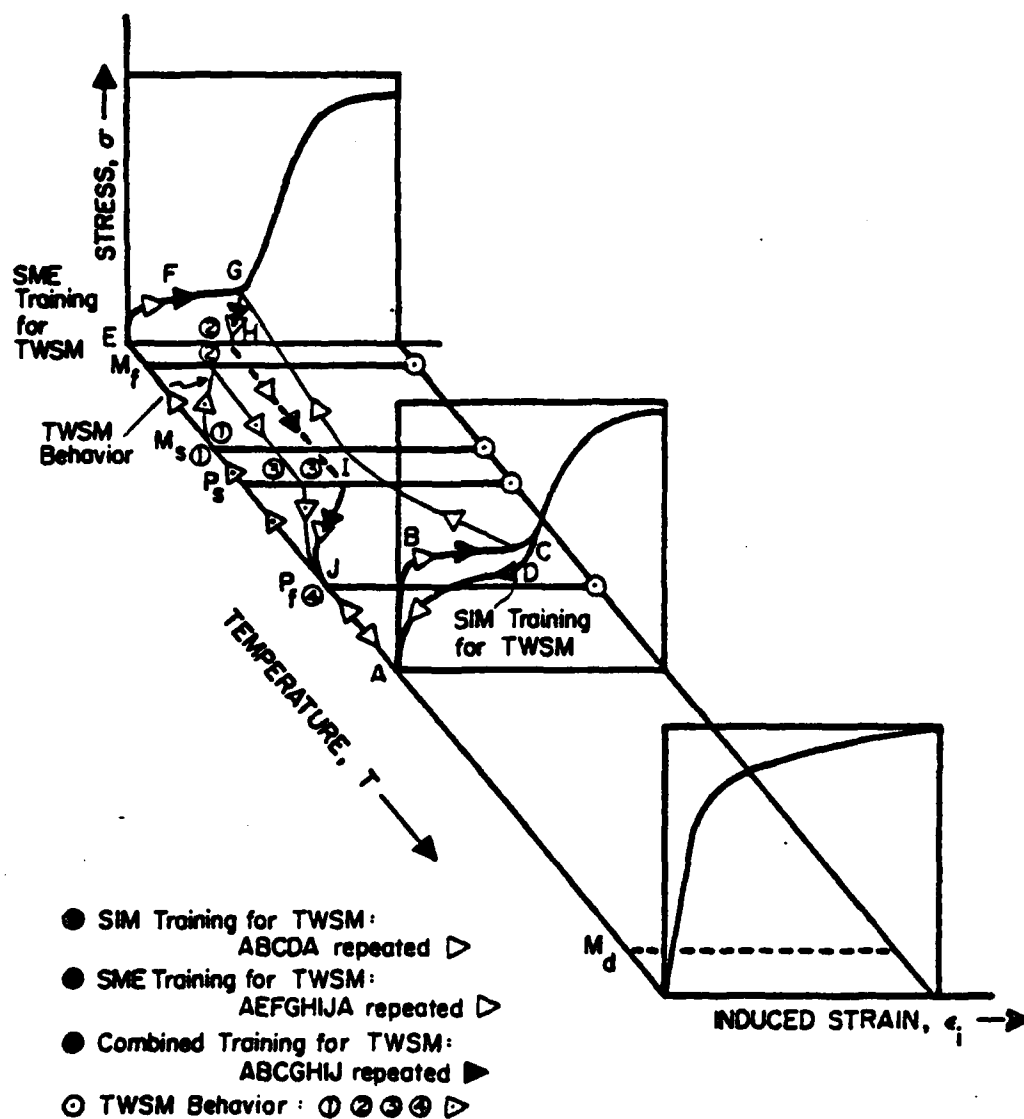


Figure 1. Schematic illustration of training routines used to obtain two-way shape memory (TWSM) behavior; SIM training for TWSM involves repeating the pattern ABCDA; SME training for TWSM involves repeating the pattern AEF GHIJA; "combined" training for TWSM involves repeating the pattern ABCGHIJA. After training the alloy will spontaneously follow the TWSM behavior pattern ① ② ③ ④ on cooling and heating.

shape memory with increasing training and whether a point of diminishing returns is reached in such training.

Finally, this work is concerned with documenting sub-microstructural changes as a function of training cycles in an effort to gain an understanding of the mechanisms of two-way shape memory.

II. EXPERIMENTAL PROCEDURE

A. ALLOY PREPARATION

The Cu-Zn-Al alloys studied were provided by Delta Materials Research Limited, Ipswich, Suffolk, England. Alloy designator D was used exclusively for this research. Its nominal composition is 69.25 wt.% Cu, 26.75 wt.% Zn and 4.0 wt.% Al. This alloy was selected on the basis of its reputed M_s temperature, which would place it in the parent phase at room temperature. The as-received material was machined into tensile test specimens dimensioned at 2.250 inches (57.15 mm) in length and 0.1378 inches (3.5 mm) uniform diameter. In order to homogenize the tensile test specimens, the specimens were sealed in evacuated quartz tubes and solution treated. The solution temperature was determined from phase diagrams in Ref. 4. The specimens were annealed at 900°C for 15 minutes and quenched in ice water. They were subsequently microscopically examined and found to consist of homogenous parent phase with a large grain structure, about 0.3 mm in diameter. Each tensile test specimen was hand polished followed by electropolishing in 10% KCN solution (6 V. a.c. for 30 S.).

B. TRANSFORMATION TEMPERATURE DETERMINATION

Small disks of the alloy, 3.5 mm in diameter and 0.030 mm thick were cut, sealed and solution treated for use in determining

martensite and parent start and finish temperatures. A single disk was subjected to thermal cycles in a Perkins-Elmer Corporation Model DSC-2 Differential Scanning Calorimeter (DSC).

The DSC provides a measure of the rate of release or absorption of energy of transformation and so allows a determination of the temperatures at which the transformations start and finish.

The temperatures recorded for alloy D are as follows:

Parent Start (P_s)	264 $^{\circ}$ K
Parent Finish (P_f)	279 $^{\circ}$ K
Martensite Start (M_s)	268 $^{\circ}$ K
Martensite Finish (M_f)	253 $^{\circ}$ K

C. ALLOY TRAINING APPARATUS AND PROCEDURE

Training routines were conducted on an Instron Testing Machine, Model 1102 TM-S-L at a constant strain rate of 0.008 in/min. A 1.0 inch specimen gauge length was used. The grips were manufactured at this facility. They were drilled and tapped to provide a serrated gripping surface and then slit to permit constriction of the specimen when collar screws were tightened. Preliminary tests were conducted to ensure non-slippage of the grips while providing uniform strain along the length of the tensile test specimens.

Surrounding the grip assembly and test specimen was an insulated bucket which could be raised or lowered on the lower grip and into which, liquids at various temperatures could flow via a simple siphon system. In order to cycle alloy D between the martensite and parent phases, a mixture

of methyl alcohol and liquid nitrogen was used to achieve the low temperature phase while room temperature alcohol was used for the high temperature phase. Temperature was determined by means of a Newport Laboratories pyrometer, Model 267B-KC1, coupled to a chromel/alumel thermocouple.

Strain and training response was measured at the grips by means of a non-contact Electro Corporation Electro-Micrometer Model PA11547, which was mounted on extension arms to remove it from the liquid in the bucket. The output from the "electromic" was fed to a Honeywell Electronik 194 strip chart recorder. Figure 2 is a photograph of the experimental apparatus. Figure 3 shows the grips, specimen and electromic sensor arrangement.

The general training routine for the specimens consisted of the following sequence:

- (1) Starting with alloy in the parent phase ($T > P_f$) strain 3%.
- (2) While maintaining strain, cool specimen below M_f .
- (3) Unload by moving Instron crosshead to achieve zero stress.
- (4) Unfix one end by removing pin from upper grip.
- (5) Warm to $T > P_f$.

This routine corresponds to the path ABCGHIJ in Figure 1.

This sequence was conducted for various number of cycles. Evaluation of TWSM after a given number of training cycles consisted of the following sequence:

- (1) Starting with the trained alloy in parent phase ($T > P_f$) and upper grip unfixed.

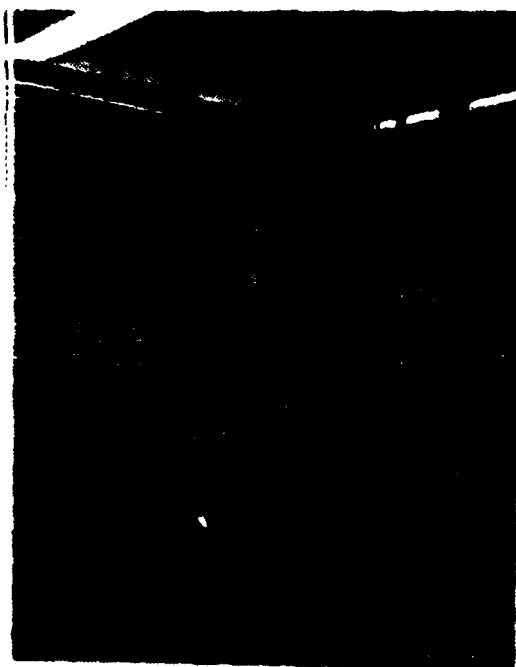


Figure 2. Experimental Apparatus



Figure 3. Grip Assembly and Sensor Arrangement

(2) Cool to $T < M_f$, record displacement.

(3) Warm to $T > P_f$, record displacement.

It should be noted that while the upper grip was unpinned and thus the specimen free to move, the upper collar remained in place. This collar exerted a force of 0.5lbf thus requiring the specimen to generate an internal reversion stress of approximately 35 psi* before any displacement would occur. Based on studies of reversion stress generated in other alloys (NiTi) [Ref. 5] this is considered a very small value and in any event was consistent for each specimen trained and tested.

D. DIFFERENTIAL SCANNING CALORIMETER RETESTING

After training, the specimens were rerun in the DSC in order to determine any shift in parent and martensite temperatures.

E. TRANSMISSION ELECTRON MICROSCOPY

Disks were cut from trained tensile specimens and prepared by jet polishing in a 3% percloric/methanol solution using Struers Tenupol 2 apparatus.

For follow-on studies using this polishing technique, some advice is in order. Considerable time was spent attempting to achieve a satisfactory TEM specimen. Best results were obtained when the solution temperature was -40 to -50°C and the jet speed was very low, 0.5 on the apparatus used. Frequent change of solution is required. Once the solution discolors, it requires changing.

*To convert psi to Pascals multiply by 6894.575.

The finished foils were examined and photographed with a Philips Corp. EM 201 transmission electron microscope. Foils were examined prior to and after various number of training cycles in order to observe changes in microstructure that might help characterize the training mechanism.

III. RESULTS AND DISCUSSION

A. DESCRIPTION OF THE TRAINING ROUTINE

A schematic representation of the type of training routine used in this research is depicted as ABCGHIJ in Figure 1 taken from Ref. 1. The experimental results generated in this work in general confirm the shape of this curve, with some exceptions. For clarity, Figure 4A and 4B are presented. These figures are representative of the data generated during the actual training routine. Figure 4A depicts the Instron machine stress vs. crosshead movement plot while Figure 4B is representative of the electronic displacement data from the Honeywell strip chart recorder.

A distinction should be made between the first training cycle and subsequent cycles. During the first training cycle, the peak stress level, Figure 4A point B, for the initial deformation via the stress induced martensite mechanism (SIM) was greater than in a typical follow-on training cycle (pt.F). As will be discussed later the peak stress level for a given initial deformation was a decreasing function of the number of cycles. Once the desired initial induced displacement Δ_i , was reached, the Instron machine was stopped. While maintaining the grips in this fixed position, chilled methanol ($T < M_f$) was siphoned into the bucket surrounding the specimen. When

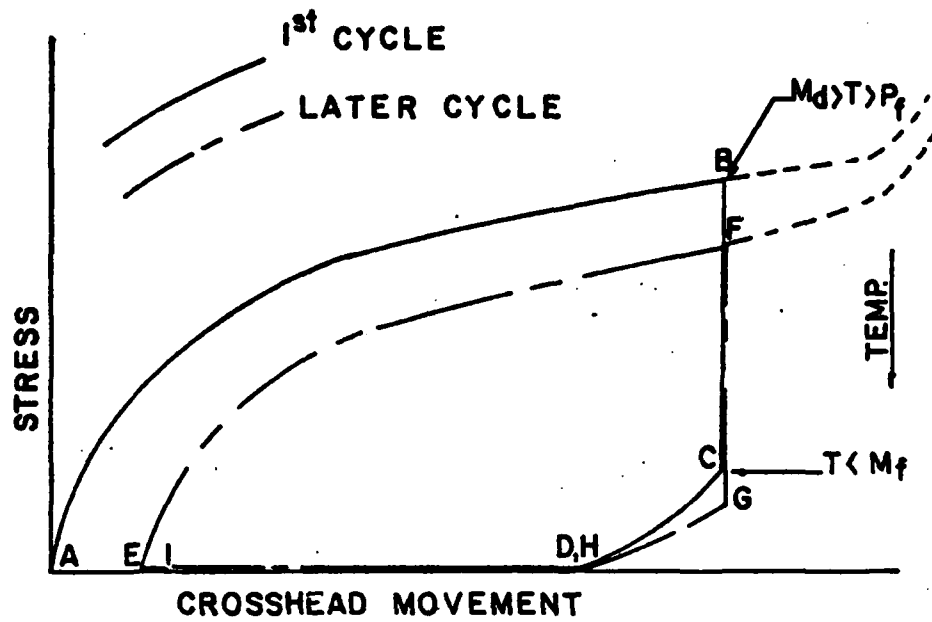


Figure 4A. Typical Instron Chart Recording

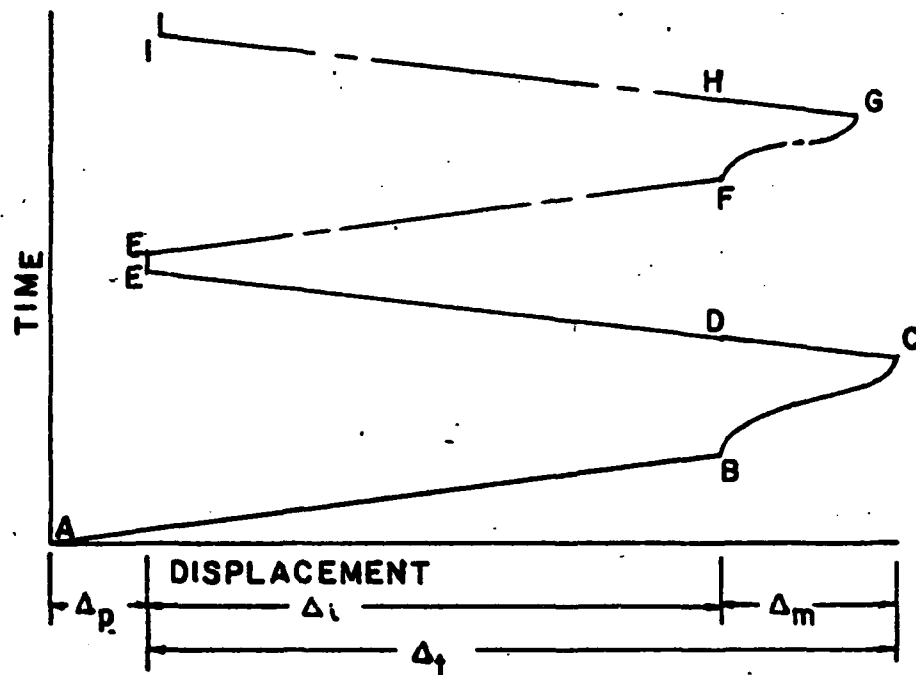


Figure 4B. Typical Displacement Chart Recording

this was done, the stress level dramatically decreased, pt. B→C, Figure 4A, while the elongation simultaneously increased, pt. B→C, Figure 4B. This elongation, due to formation of thermoelastic martensite under stress is designated Δ_m . After a short period of time, this thermoelastic martensitic transformation is complete, at pt. C. In essence, the specimen, at pt. C, has undergone a stress induced martensitic transformation with a thermoelastic martensitic transformation superimposed upon it. It is this low temperature, low stress, maximum elongation point that the specimen is being trained to remember. From pt. C the crosshead was moved to achieve a zero stress level. With this accomplished, the specimen, unfixed at one end and heated to $T > A_f$, returned to the vicinity of its starting shape.

Of particular note during the first training cycle was the imparting of some amount of irreversible plastic deformation to the specimens. Amounts of initial plastic deformation (Δ_p) per 1000 mil gauge length specimen are given in Table I.

Table I

Amount of Plastic Deformation (Δ_p) Retained in the Specimen after the First Training Cycle (in mils)*

Specimen Designation	D-10	D-5	D-3	D-4	D-9	D-6	D-7
Eventual Training Cycles	(3X)	(5X)	(10X)	(15X)	(20X)	(20X)	(30X)
Δ_p	6.6	8.4	6.6	13.8**	3.0	2.4	6.0

*Since the specimen's original gauge length was 1 inch or 1000 mils, Δ_p , first cycle, can be converted to % plastic strain by dividing table entries by 10. For example, first cycle % plastic strain for specimen D-10 would be 0.66%.

**First two cycles.

The cause of this deformation may be due, in part, to slight misalignment of the Instron machine. More likely, however, there has been stress accommodation at β (parent phase) grain boundaries which separate grains of different orientation. In effect, the strain limit for completely reversible shape memory (ϵ_L) has been exceeded in local areas of the polycrystalline material. In any event, it is clear that some points within the specimen experience irreversible plastic deformation. Nagasawa [Ref. 6] has suggested a necessary condition of TWSM is severe deformation below M_s , while Otsuka [Ref. 7] notes that by inducing plastic strain you assist the stress induced martensite transformation. Otsuka explains that dislocations introduced by the plastic strain assist nucleation of a particular variant of stress induced martensite. Perkins [Ref. 8] notes that the most pronounced TWSM effects are observed in cases where an alloy is deformed severely and nonuniformly, such that some fibers exceed the strain limit, (ϵ_L).

The starting point for each subsequent training cycle is the final elongation of the previous cycle. In Figure 4B, point E is the point of elongation after completion of the first training cycle. Point E then becomes the starting point for training cycle number two.

3. TRENDS IN TRAINING CYCLE PARAMETERS AS A FUNCTION OF THE NUMBER OF CYCLES

Before presentation of parameter trends a note of caution is in order. As originally conceived, the purpose of the

research was to consider the training effects resulting from subjecting a specimen to a number of SIM/SME cycles. As such, it was necessary, during the training cycle, to effect a phase change from parent to martensite phase. The necessary condition was the phase change and not the exact and repeatable temperature level of the phase change. While the experimental cyclic temperatures were kept close during each training cycle, they were not exactly repeated. In the following analysis, where parameters are known to be temperature sensitive, such as stress, trends will be established for a particular temperature. For other parameters, like strain, which has been shown not to be strongly temperature sensitive, the data is presented with the aforementioned caveat in mind.

1. Induced Displacement

The displacement change introduced into the specimen by crosshead movement (Δ_1) is tabulated in Table II and presented graphically in Figures 5-7 for specimens D-6,9,7. A first cycle induced strain of 3% was selected. Ref. 4 lists this strain as an acceptable one for polycrystalline material. The Table II entries for the first cycle subtract the amount of first cycle plastic deformation listed in Table I. That is, Table I plus Table II first cycle entries equal 3% strain or 30 mils. As can be seen from the Table, the amount of successive induced displacement decreases as cycles are increased and approaches some constant level. This decrease in induced displacement was approximately 4 to 5 mils in the

Table II
Induced Displacement (Δ_i) in mils

<u>Cycle</u>	<u>D-10</u>	<u>D-5</u>	<u>D-3</u>	<u>D-4</u>	<u>D-9</u>	<u>D-6</u>	<u>D-7</u>
1	23.4	21.6	23.4	19.2	27.0	27.6	24.0
2	23.4	21.6	24.0	27.0	27.0	28.2	24.6
3	23.4	20.4	22.2	27.0	25.8	27.6	24.0
4		20.4	22.8	26.4	25.2	27.0	24.0
5		19.8	22.8	24.6	24.6	26.4	24.6
6			21.6	25.8	24.6	26.4	23.6
7			22.3	24.6	24.6	25.2	24.0
8			21.0	25.2	22.8	25.2	24.0
9			21.6	24.6	24.0	24.0	24.0
10			22.2	23.4	24.0	24.0	22.8
11				22.2	23.4	23.7	22.8
12				22.8	23.4	22.8	23.4
13				22.2	23.4	22.8	24.4
14				22.2	23.4	22.8	23.1
15				22.2	24.4	22.8	24.4
16					24.0	22.8	22.2
17					23.4	21.0	23.7
18					23.4	21.6	23.7
19					23.4	21.6	22.2
20					23.4	22.2	22.2
21							21.6
22							22.2
23							22.2
24							22.2
25							22.2
26							21.0
27							21.0
28							21.9
29							21.6
30							22.8

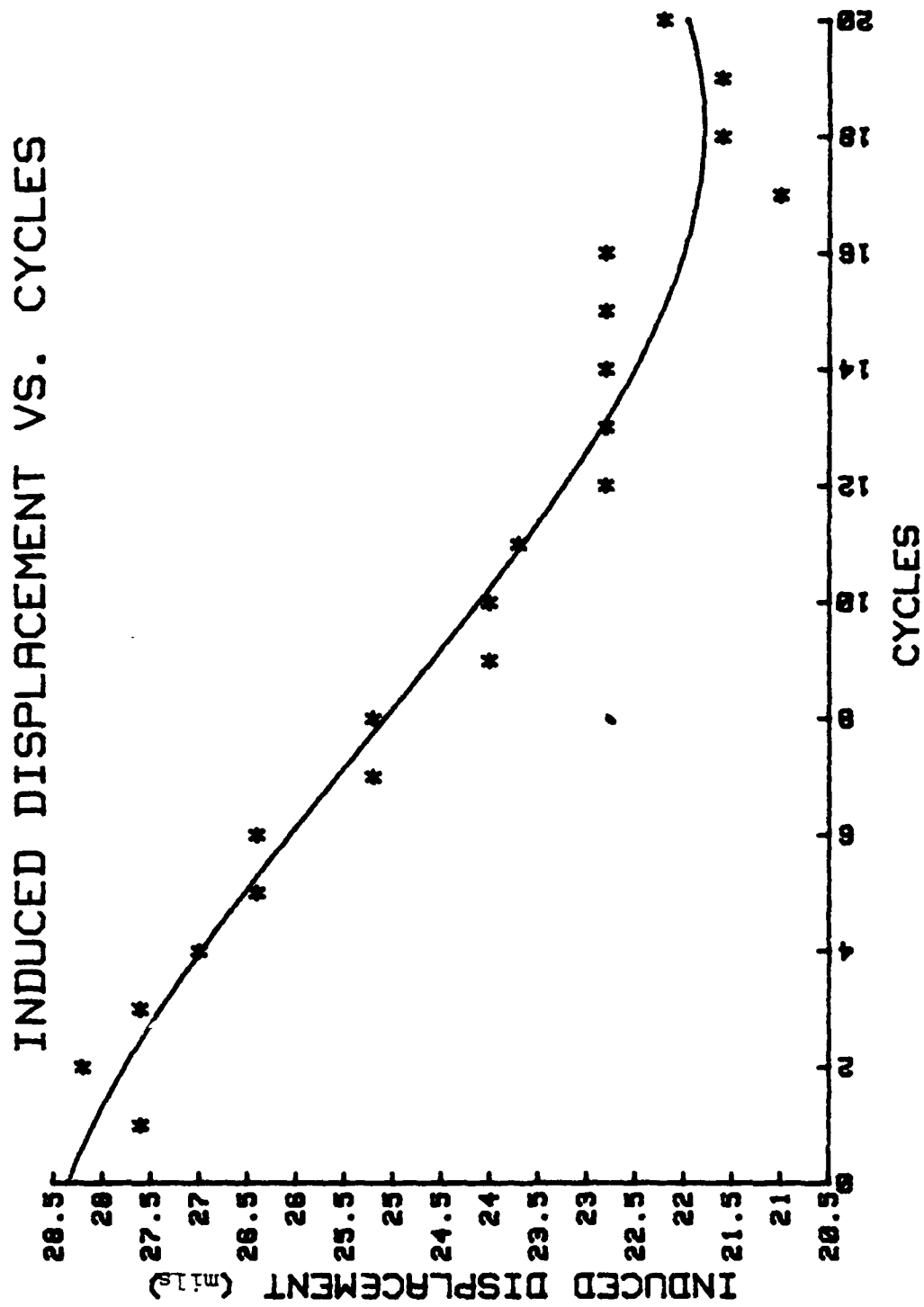


Figure 5. Specimen D-6 (20 training cycles)

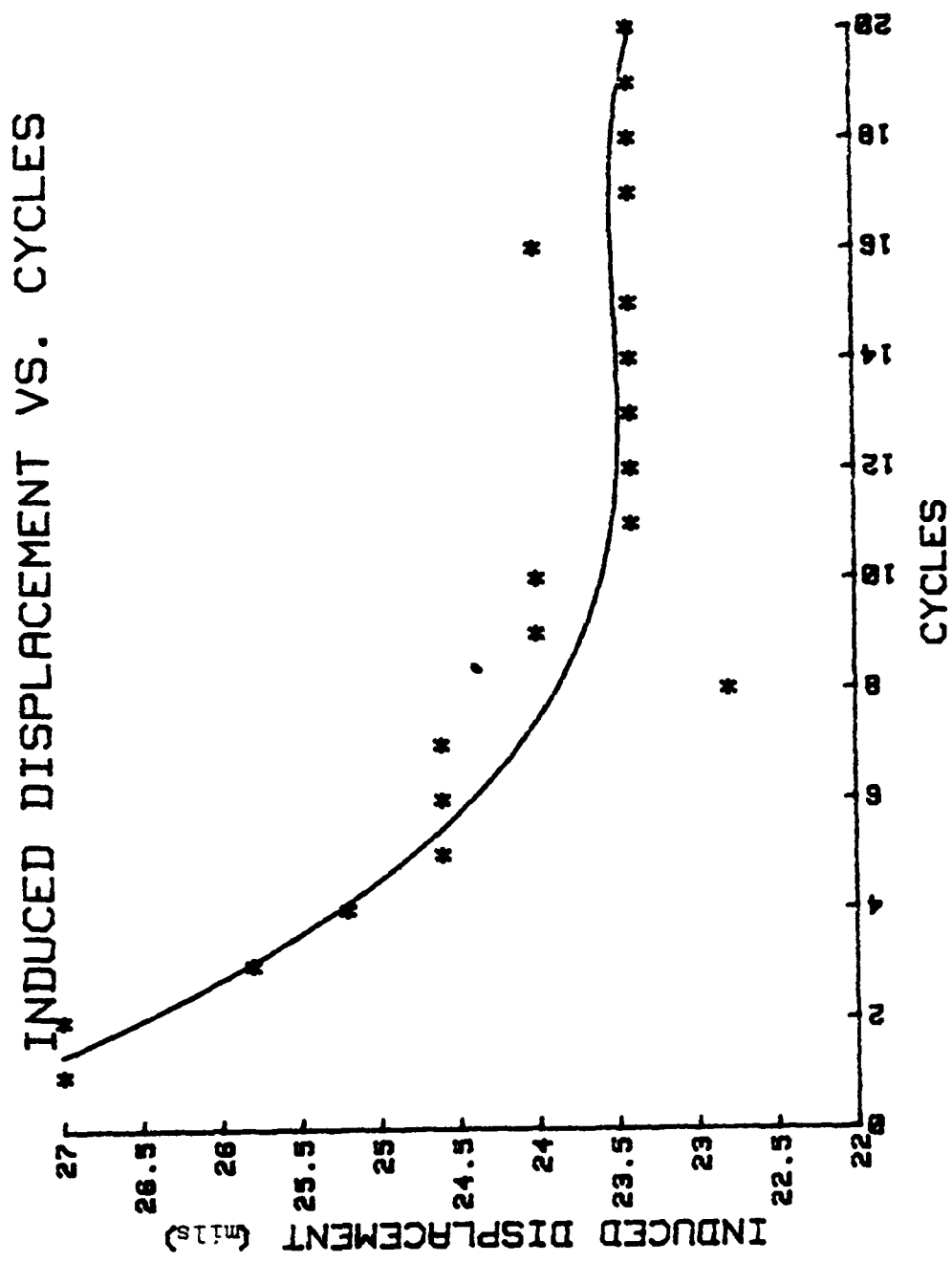


Figure 6. Specimen D-9 (20 training cycles)

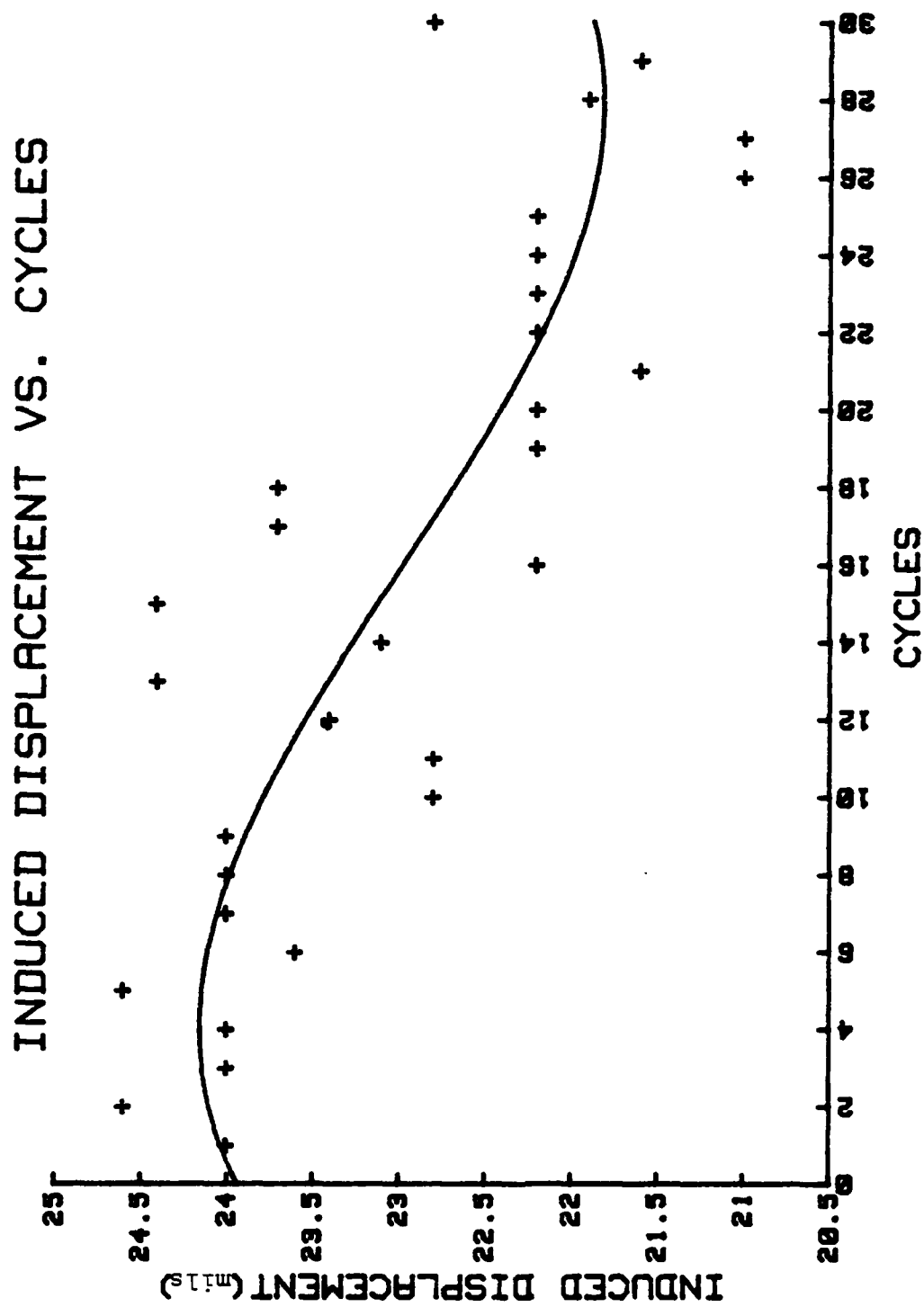


Figure 7. Specimen D-7 (30 training cycles)

highly trained specimens (D-4, D-9, D-6, D-7). It is speculated that the source of this downward trend is two-fold. First, some small amount of additional plastic deformation could be occurring. That is, a strain hardening condition could be achieving saturation. Secondly, it is possible that the alloy begins to "remember," via microstructural change, its strained low temperature position and thus does not fully recover its initial positions upon heating to $T > A_f$. One possible microstructural mechanism for this unwillingness of the specimen to recover its original position is the retention of small, but increasing amounts of retained martensite. During experimentation, it was possible to partially drive the alloy back to its previous cycle displacement starting position by increasing the temperature of the bath. Thus both the possibility of additional plastic deformation and the retention of some amount of metastable retained martensite is likely. Delaey [Ref. 9] has found retained martensite appears both on thermal and stress cycling. Muesing [Ref. 10] has made similar findings in the case of thermal cycling.

2. Elongation due to Thermoelastic Martensitic Transformation under Stress

Table III lists elongation recorded due to Δ_m . It can be seen that the elongation occurs to the greatest extent in the first or second cycle and drops to a fairly constant value with a small declining bias. It should be remembered

Table III

Thermoelastic Martensitic Displacement (Δ_m) in mils

<u>Cycle</u>	<u>D-10</u>	<u>D-5</u>	<u>D-3</u>	<u>D-4</u>	<u>D-9</u>	<u>D-6</u>	<u>D-7</u>
1	6.6	9.6	7.2	7.2	7.2	6.6	7.2
2	5.1	7.5	4.2	3.6	7.2	7.8	5.4
3	5.1	7.2	4.8	4.5	7.2	6.6	5.4
4		7.5	4.8	4.8	5.4	7.2	4.8
5		7.2	4.8	4.8	6.0	7.2	5.4
6			5.0	4.2	6.0	6.9	4.8
7			4.2	6.0	6.0	6.9	5.4
8			3.6	6.0	4.2	6.0	5.4
9			3.6	5.4	5.4	5.4	6.6
10			4.2	6.6	4.8	5.4	4.8
11				6.0	4.8	6.6	4.8
12				6.6	4.8	6.6	4.8
13				4.8	4.8	5.4	5.4
14				5.1	4.2	6.0	4.8
15				4.2	4.8	4.8	5.4
16					5.4	4.2	5.4
17					4.8	4.2	6.0
18					4.8	4.2	6.0
19					5.4	4.2	7.2
20					5.1	5.4	4.8
21							6.0
22							6.0
23							5.4
24							6.0
25							6.0
26							5.4
27							4.2
28							5.1
29							3.6
30							5.4

that at this point in the training cycle the Instron machine crosshead is fixed. In order for the specimen to elongate at all, its displacement must be accommodated by the Instron/grip assembly, either by thermal contraction or machine compliance. Since the observed stress decreases dramatically during the thermoelastic martensite transformation, rig thermal contraction alone is ruled out. It is likely that slight deflection of the load cell accommodates the small displacements associated with Δ_m . Since the stress level does not reach zero, additional Δ_m would be possible if the specimen was inclined towards greater displacement.

3. Total Elongation

The trained elongation, designated Δ_T , is the sum of the induced elongation and the thermoelastic elongation. It is this displacement which will be used as a base to compare trainability of specimens.

4. Peak Stress at Fixed Temperature

Figure 4A points B and F are designated peak stress points for a particular cycle. Table IV lists peak stress values as a function of cycles at fixed temperature for specimens D-3, D-4, D-6, D-7, D9. Figures 8, 9, 10 are a graphical representation for specimens D-3, D-6 and D-9. The temperature for the stress listings was 10°C, except for specimen D-4 where it was 11°C. The peak stress, in general, decreases as the number of training cycles increases. The magnitude of this decrease is of the order of 1000-2000 psi.

Table IV
Peak Stress at Fixed Temperature

<u>Alloy</u>	<u>Cycle</u>	<u>Peak Stress (psi)*</u>
D-3	2	12,800
	3	12,533
	4	12,800
	5	11,733
	6	11,733
	7	11,266
	9	11,733
	10	11,266
D-4	2	20,000
	6	17,666
	7	16,000
	11	15,066
	13	15,466
D-6	1	15,825
	4	15,090
	9	13,745
	11	13,611
	13	13,142
	15	12,875
	16	12,807
	18	12,800
D-9	3	18,305
	4	17,770
	7	18,230
	10	16,300
	11	15,825
	13	15,757
	15	15,020
	18	15,623
	20	15,220

*To convert psi to Pascals multiply by 6894.575.

Table IV (cont'd)

<u>Alloy</u>	<u>Cycle</u>	<u>Peak Stress (psi)</u>
D-7	2	13,670
	3	13,600
	5	14,000
	10	14,333
	12	13,333
	14	12,800
	17	13,866
	19	14,800
	22	14,333
	23	13,333
	24	14,800
	26	13,333
	27	12,666
	28	12,133
	29	11,670

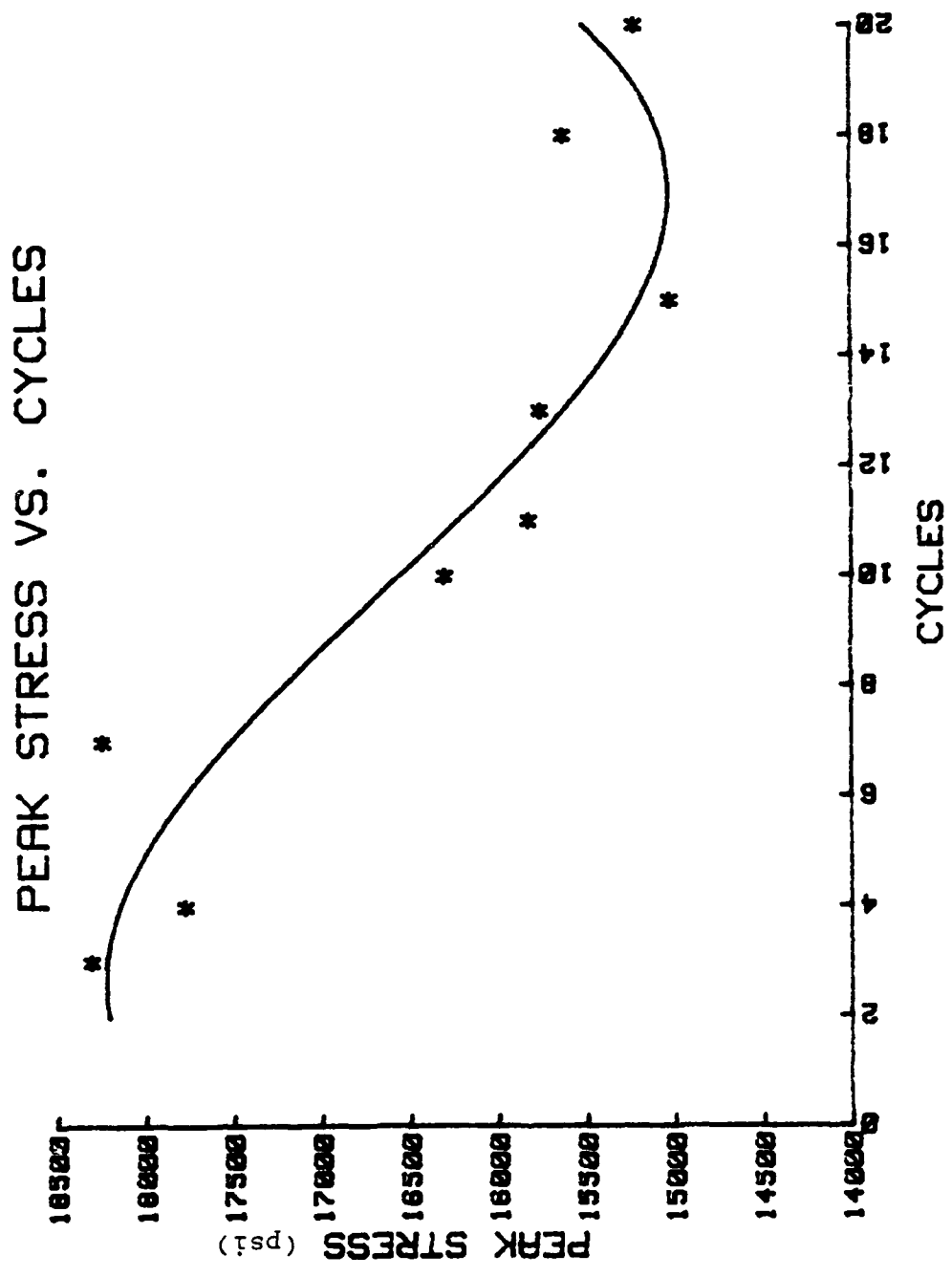


Figure 8. Specimen D-3 (10 training cycles)

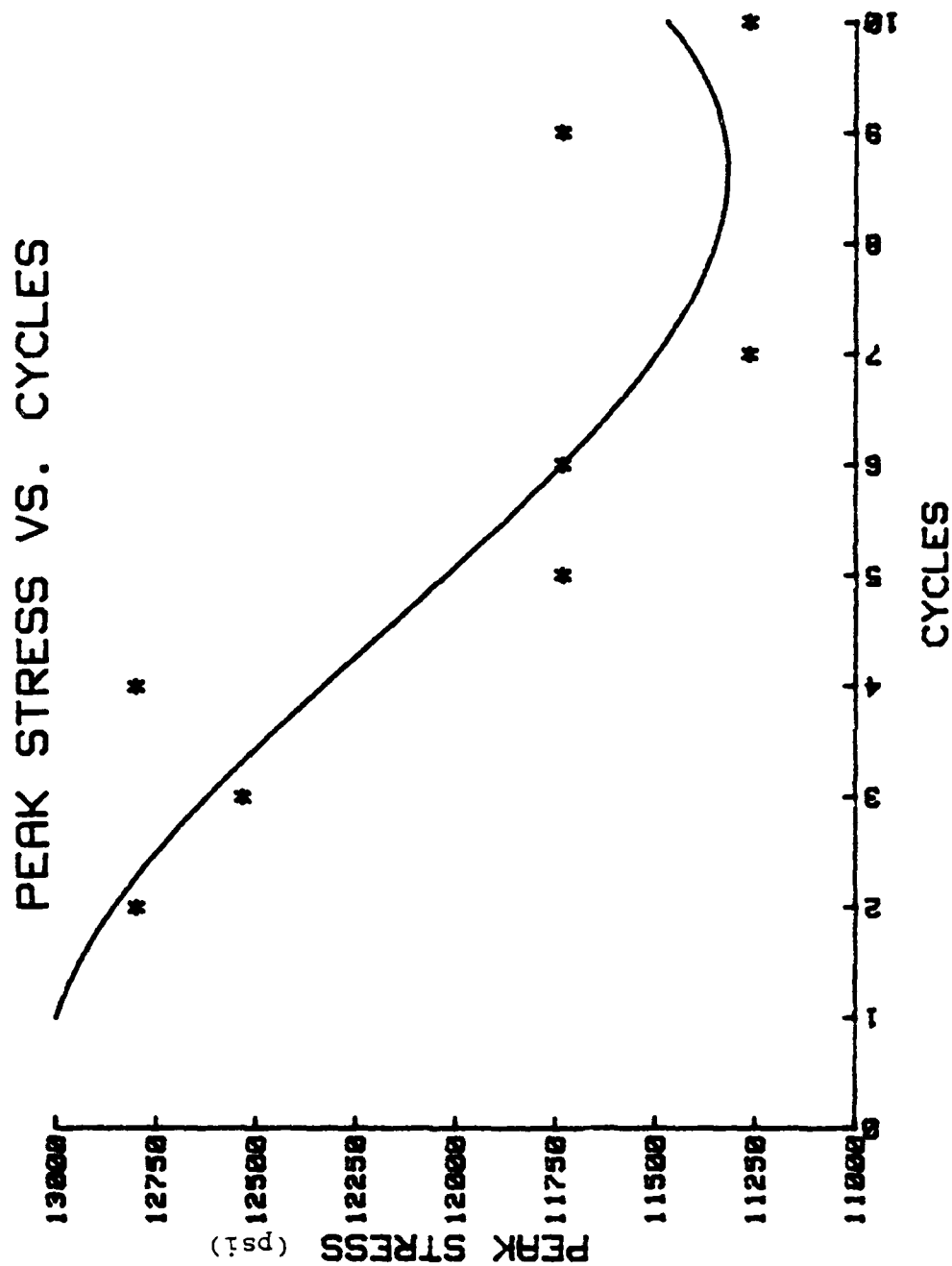


Figure 9. Specimen D-6 (20 training cycles)

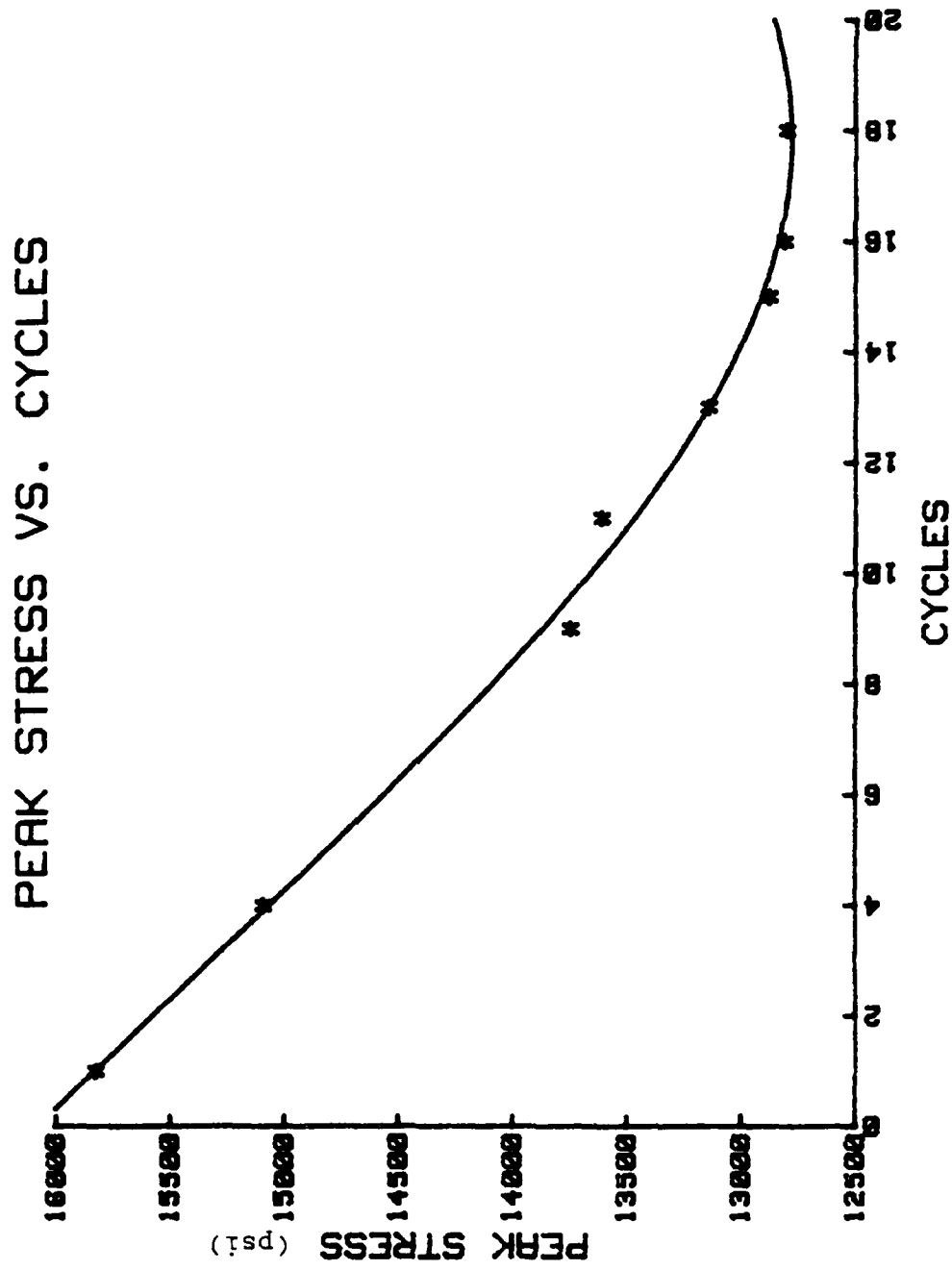


Figure 10. Specimen D-9 (20 training cycles)

An objection might be raised at this point that the amount of induced elongation (Table II) decreases as the number of cycles increases and so one would expect peak stress to decrease. Three points are important in the respect. First, Hookes Law does not apply to this area of stress/displacement curve for a shape memory alloy. That is, the formation of stress-induced martensite leads to a distinctly non-linear relationship. Second, even if elongation of the same magnitude, at the same temperature at different training cycle points are compared, a decreasing bias in peak stress remains. Finally, it is fairly certain that some amount, albeit small, of plastic deformation is occurring as cycles increase and therefore one would expect peak stress to increase, not decrease.

It is possible that the alloy, by microstructurally adjusting to the training routine, is able to achieve its maximum elongation at lower stress as training proceeds. Schroeder and Wayman [Ref.11] have concluded that TWSM results from a preferred variant of martensite, that variant which permits the lowest stress to be obtained. K. Otsuka [Ref. 7] has found that after permanent strain was introduced, the stress for forward transformation was lowered. That is, the introduction of strains assist the transformation.

5. Training Cycle Comparisons

Table V lists data concerning values at various cycle points. Peak stress has been previously defined.

Table V

Training Cycle Parameters - Typical Beginning and Ending Values

Alloy	Cycle	σ_{max} (psi)	σ_{cool} (psi)	Start Temp. (°C)	Cool Temp. (°C)	Δi (mils)	Δ_m (mils)
D-3	2	12,800	2,335	10	-33	24.0	4.2
	10	11,266	1,000	10	-31	22.2	4.2
D-4	3	20,000	8,660	12	-34	27.0	4.5
	13	15,530	5,330	12	-34	22.2	4.8
D-6	1	15,825	2,550	10	-30	27.6	6.6
	2	16,760	2,350	12	-40	28.2	7.8
	20	14,080	805	12	-40	22.2	5.4
D-9	1	18,775	4,025	12	-40	27.0	7.2
	4	17,770	5,630	11	-40	25.2	6.0
	20	15,220	3,350	11	-40	23.4	5.1
D-7	1	16,600	2,666	10	-38	24.0	7.2
	2	13,670	1,000	9	-43	24.6	5.4
	29	11,670	500	10	-43	21.6	3.6

Cooling stress (σ_{cool}) corresponds to the stress level after the specimen has transformed from parent to martensite (points C or G, Figure 4A). Start temperature is the temperature that the specimen experienced during the formation of stress induced martensite (points A+B, Figure 4A). Cooling temperature is the temperature at which formation of thermoelastic martensite took place (points B+C, Figure 4A).

The specimen cycle numbers were selected in order to compare values at similar temperature for early and concluding cycles. In general, the parameters decrease in value as the number of cycles increases. It is thus apparent that the alloy is learning its training routine. The elongation due to the thermoelastic martensitic transformation decreases because, after the first few cycles the alloy retains some amount of martensite and therefore less is available to transform.

C. TWSM TRAINABILITY RESULTS

Table VI displays data concerning the ability of the specimens to demonstrate TWSM as a function of the number of training cycles to which they were subjected. The percentage entries in the table are a ratio of the displacement recorded during a test sequence, designated Δ_{TWSM} , (see Experimental Procedure) divided by the average total displacement (Δ_T) over the cycles previous to the testing cycle ($\Delta_{TWSM}/\Delta_T \times 100$). That average displacement, in mils, is the figure in parenthesis

Table VI

TWSM Performance

Alloy	Number of Training Cycles									
	3	5	10	13	15	18	20	25	28	30
D-10	10.4% (29.0)									
D-5		27.3% (28.6)								
D-3			45.6% (29.1)							
D-4					49.5% (29.1)					
D-9							34.4% (29.6)			
D-6		33.9% (34.4)	38.5% (32.8)				45.7% (30.2)			
D-7		20.2% (29.8)	30.6% (29.4)	40.1% (29.2)	45.2% (29.2)	43.3% (29.1)	43.4% (29.0)	47.9% (28.8)	47.3% (28.5)	48.6% (28.4)

under the percentage entry. In this respect, the percentage trainability of the specimens is a conservative estimate. The TWSM test displacement, Δ_{TWSM} , recorded after a specified number of training cycles is an absolute number recorded as a function of temperature change. The denominator, Δ_T , on the other hand, must represent the amount of displacement trained into the specimen and is a moving average which incorporates greater displacements in earlier cycles.

Because the alloys were to be subsequently examined in the Transmission Electron Microscope specimens D-10, D-5, D-3, D-4 and D-9 were trained to a specific target cycle and evaluated only at that end point. Specimen D-6 and D-7 were trained and evaluated at various intervals along the way to supply additional data on TWSM trainability.

Figures 11 and 12 display TWSM results graphically. Figure 11 is a composite graph fitting all TWSM data in Table VI with a third order polynomial. Average % TWSM values are used for training points where multiple data exists, i.e., 5, 10, 15, 20 cycles. Figure 12 displays results for specimen D-7.

The data indicates that subjecting the alloy to increasing numbers of training cycles has a definite effect on the alloy's ability to demonstrate increasing displacements during tests of TWSM. Perhaps result of specimen D-7 best demonstrates the ability to train shape memory alloys. In

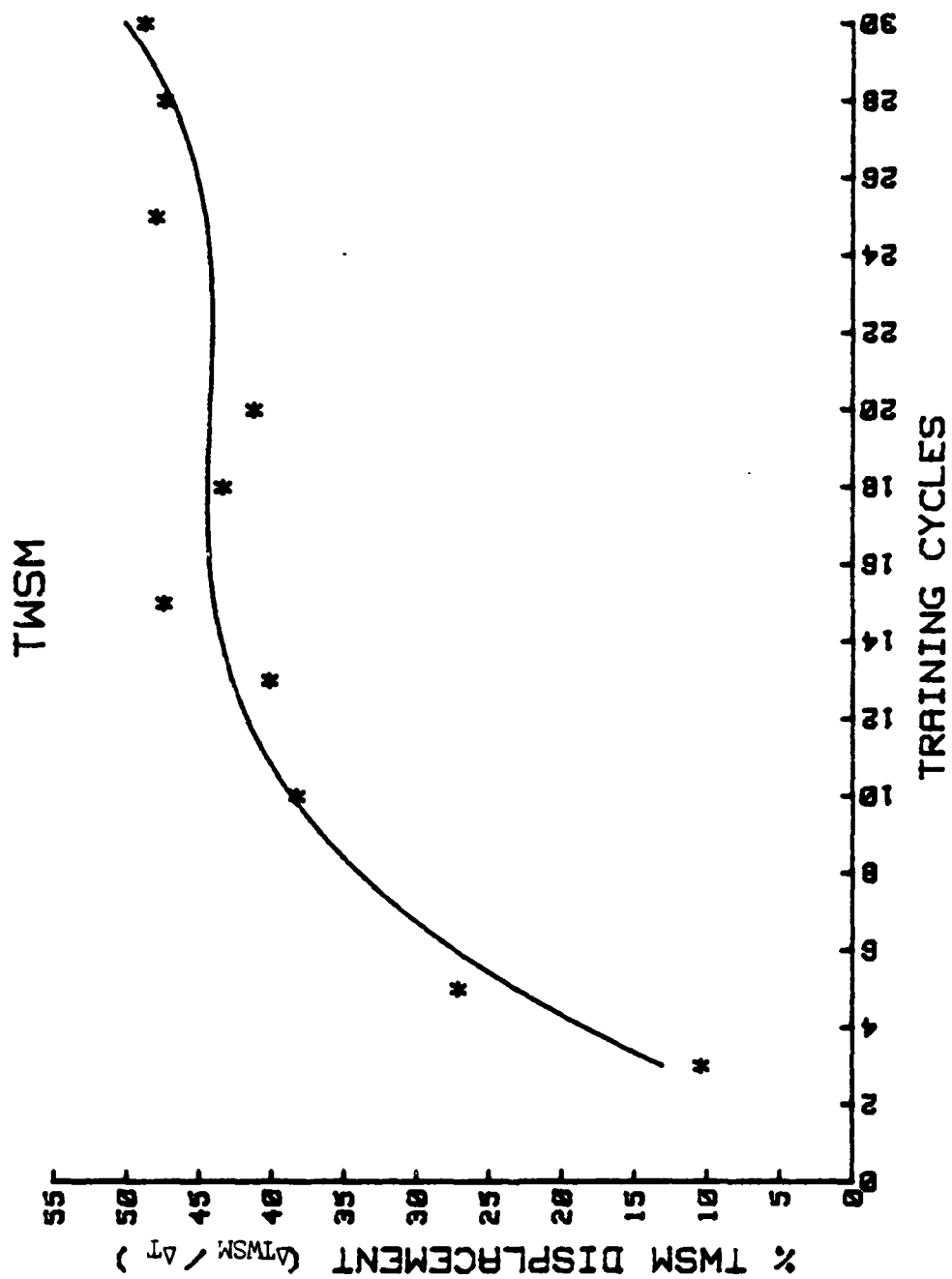


Figure 11. TWSM Trainability Results Composite

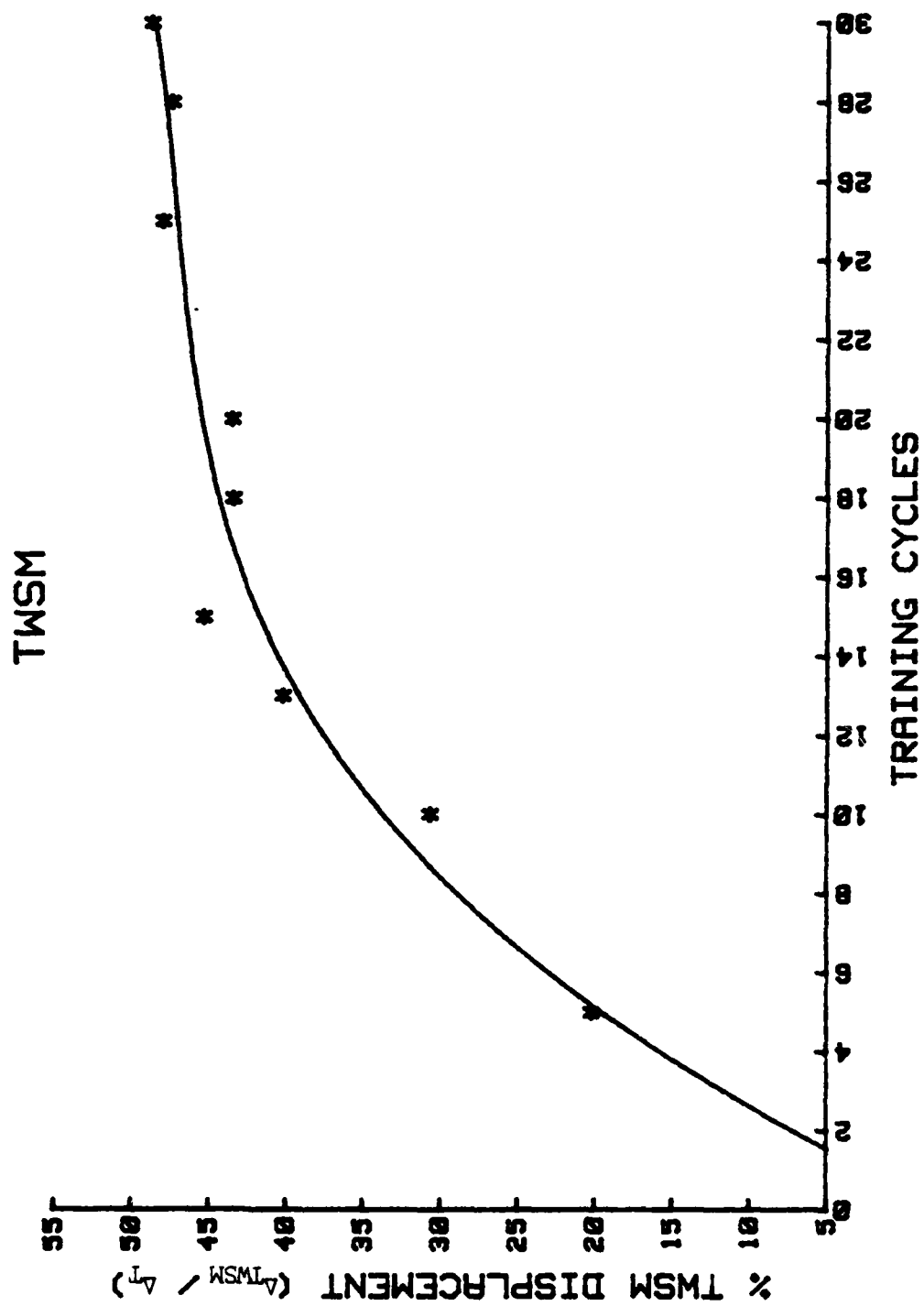


Figure 12. TWSM Trainability Results Alloy D-7 (30 training cycles)

general, D-7 was able to achieve greater displacements during TWSM tests as the number of training cycles increased. During early testing of D-7 (<18 cycles) this specimen showed a tendency toward greater displacement on cooling to $T < M_f$ than, during the same test, to heating $T > A_f$. These unequal TWSM displacements ceased during later tests. Between cycles 15 and 18, a small drop in trainability is observed. It should be noted that, due to the length of the training routine (30 cycles) for D-7, it was conducted over a two-day period. In general, however, the trained alloys were able to repeat their trained displacement over a series (up to 5) of thermal cycles and to repeat their training after a period of time. For example, alloy D-5 was retested after six days and was able to demonstrate no loss of TWSM.

Specimen D-9 demonstrated a low amount of training after 20 cycles. The reason for this poor performance is unclear. It is speculated that its low first cycle plastic deformation (3.0 mils) may be a factor. It is also possible that alloys can in effect "overtrain" and decrease performance as training cycles increase, although this was not the case with other specimens.

D. DIFFERENTIAL SCANNING CALORIMETER DATA

Table VII provides data on parent and martensite start/finish temperatures and how these vary for the trained specimens. Two table entries for each transformation temperature

Table VII

DSC Data

<u>Specimen</u>	<u>M_s(°K)</u>	<u>M_f(°K)</u>	<u>P_s(°K)</u>	<u>P_f(°K)</u>
D-11 (untrained)	268	253	264	279
D-11 after 6 DSC thermal cycles	268	253	264	279
D-10 (3X)	266	251	263	278
D-10 after 6 DSC thermal cycles	267	251	263	278
D-5 (5X)	263	248	262	276
D-5 after 6 DSC thermal cycles	265	249	262	276
D-3 (10X)	268	253	266	279
D-3 after 12 DSC thermal cycles	271	252	266	279
D-4 (15X)	266	252	267	279
D-4 after 12 DSC thermal cycles	269	254	267	279
D-6 (20X)	265	250	264	278
D-6 after 12 DSC thermal cycles	267	251	265	278
D-7 (30X)	261	244	258	274
D-7 after 12 DSC thermal cycles	263	245	259	274

are provided. The first entry reflect data from the first DSC thermal cycle. The second entry provides that same parameter value after 6 or 12 DSC thermal cycles, as indicated.

There appears to be no identifiable trend as a function of training cycles. Specimen D-5 and D-7 M_s and M_f differ by the greatest margin relative to the untrained alloy (D-11), but their P_s and P_f temperatures are low as well. This is not the case for the other specimens where P_s and P_f do not significantly vary from the untrained alloy temperatures. There is no apparent reason for the transformation temperature variance of specimen D-5 and D-7.

Findings similar to Muesing's [Ref. 8] were demonstrated in the case of DSC thermal cycling. That is, after 6 to 12 DSC thermal cycles, shift of $+1$ to $+3^\circ\text{C}$ were recorded for M_s and M_f while P_s and P_f showed little or no change.

E. MECHANISMS OF TWSM

Investigators of shape memory alloys have advanced mechanistic explanations of TWSM. Less is known about the impact of varying the number of training cycles on mechanistic TWSM routes.

Schroeder and Wayman [Ref. 11] in their work on single crystal CuZn alloys state that TWSM was observed to result from the preferential formation and reversal of a "trained" variant of martensite. The trained variant results in a single orientation where initially there were four orientations.

The authors were able, after only 2 SIM cycles, to achieve a strain offset (displacement) upon cooling equal to that during superelastic loading. In other words, the specimen has transformed to a single crystal of the preferred orientation for maximum strain upon cooling or stressing. There is reason to believe that this is occurring in polycrystalline material as well.

Delaey and Thienel [Ref. 3] present very convincing evidence in the form of a film sequence. The photographs document the changes occurring in the microstructure of a CuZnAl alloy. The authors observe the difference in microstructure between a specimen undergoing 1 training cycle and the same specimen undergoing 10 training cycles which resulted in TWSM. A specific martensite plate orientation is observed as a transition arrangement during the single training cycle photos. After completing 10 cycles, the final microstructure is virtually identical to the transition microstructure. The authors conclude that a preferred orientation distribution and growth of a particular plate variant are responsible for the spontaneous shape change associated with TWSM. One concludes that this particular martensite plate variant can be trained into the microstructure by repetition of a training regime.

Delaey in earlier work on polycrystalline alloys [Ref. 12] notes that stressing above M_s and subsequently cooling below M_f "freezes" in a particular microstructure. This will result

in large internal stresses at grain boundaries and around tapered ends of martensite plates. Upon heating, the stored energy is released and assists the martensite to β transformation.

Delaey further notes that local plastic deformation will cause residual stresses which may influence the martensite microstructure obtained in cooling the sample during training manipulations. Perkins [Ref. 13] notes that elastic back stresses, arising from plastically deformed local regions or arrays of dislocations, may partly explain TWSM. It is reasoned that successive training cycles may induce additional dislocation tangles and act as nucleation points for the preferred martensite noted by Delaey and Wayman. Otsuka [Ref. 7] has found that dislocations assist the nucleation of particular martensite variants and result in lowering the critical stress for inducing martensite.

In review, TWSM results from the development of a particular variant of martensite, and it is probably that dislocation tangles resulting from plastic deformation play a role in nucleating these preferential martensite variants by providing some amount of residual stress which assists the transformation of β to martensite. Once the martensite variant is formed by temperature change, there are stresses associated with the martensite plate arrangement which will assist the martensite to β transformation and associated shape change.

IV. TRANSMISSION ELECTRON MICROSCOPY

The microstructure of untrained alloy D is shown in Figure 13. The parent phase contains no residual martensite and no visible dislocation substructure. The mottling or tweed-like appearance of the background, observed here as well as in trained specimens, has been discussed by Delaey, Perkins and Massalski [Ref. 14] and others. Suffice it to say that it is a typical characteristic of the β parent phase.

The microstructure of alloy D after three training cycles is illustrated by Figures 14-17. It is apparent that significant changes in the substructure have occurred. Figure 14 clearly shows large numbers of dislocations, many of which adjoin a dark streak area which may be an incompletely reverted martensite plate, or an area where a plate had formed. Figures 15-17 show, in increasing magnification order, a pattern that is seen quite often in the trained specimens; the appearance of dark linear regions laying parallel to one another. Some areas between these parallel regions are featureless, while others (middle Figure 15, extreme right Figure 16) appear to have vestiges of martensite plate features, possibly dislocated martensite. Figure 17, taken at high magnification, reveals some dislocations within these martensite plate-like areas. It is probable that martensite plates resided in this region when the alloy was under stress or at low temperature,

and upon reversion to parent phase, vestiges of the plates or residual strain fields remain. Similar regions are seen in specimen D-5, trained five cycles, Figures 18 and 19. Figure 20 shows an area where martensite clearly resided. Preferential polishing has outlined the plate area. In addition, dislocations are seen at the bottom of the photomicrograph.

The microstructure after 15 training cycles is exhibited in Figures 21 through 23, from specimen D-4. These photomicrographs present a revealing picture of what may be the mechanism of TWSM. Figure 21 clearly shows an area where martensite plates resided. It appears that this region is ripe for martensite plates to form, under stress or temperature change, in this same location. That is, the martensite plates would grow into the places provided for them. In addition, under the lower plate area in Figure 21, and shown in higher magnification in Figure 22, is a parallel band which runs the length of the outlined plate area. In more highly cycled specimens of polycrystalline Cu-Al-Ni alloy, Ritter et al. found identical markings near a receding martensite plate. The author termed them "vestigial marks" [Ref. 15]. These vestigial marks may provide a banded area for the martensite plates to grow and shrink. In Figure 21 parallel arrays of dislocations are evident in the background, both between the plate areas and through the plate

areas. A high magnification photo of these dislocations is shown in Figure 23. Figure 24 shows a few distinct dislocations in the region between plates, and in the lower left, two fine retained martensite plates are evident.

The microstructure after 20 cycles, specimen D-6, is seen in Figures 25 and 26. Closely spaced light and dark regions similar to those seen in specimen D-10 and D-5 (Figures 15,16, 18,19,20) are evident. In highly trained specimens the bands are closely spaced and more prevalent. In addition, what appears to be a retained martensite plate runs through the photos. The very fine "dashed" substructure evident in the background (see lower right of Figure 26) is considered to be part of the tweed structure of the parent phase.

The microstructure after 30 training cycles is illustrated in Figures 27 to 32, (specimen D-7). In general, these photos reveal large areas of dense dislocation tangles as well as areas of retained martensite. In the center of Figure 27, there is a group of martensite plates with what appears to be dense dislocations surrounding them. Areas of retained martensite with areas of debris or vestigial marks adjoining them are clearly shown in Figure 28.

In Figure 29, at 79,500 power magnification, heavily dislocated regions adjoin apparently dislocation-free sites. The accompanying diffraction pattern, Figure 30, indicates that the area shown in Figure 29 is not purely parent phase, but may contain retained martensite in addition to parent phase.

Finally, Figures 31 and 32 display an area which appears to show dense tangles of dislocations (Figure 31). At higher magnification, 102,000X, individual dislocation lines can be distinguished (Figure 32).

A general pattern emerges from these photomicrographs. At low training cycle point, individual and quite distinct dislocations are generated as in Figure 14. Additionally, there may be residual stresses remaining in the parent phase as the stress induced and thermoelastic martensite recede with increased temperature. As training proceeds, additional dislocations are generated, which tangle and are sometimes difficult to distinguish without the aid of increased magnification. Whereas one might expect these dislocations to inhibit the formation of stress induced martensite, it has already been established that peak stress decreases as cyclic training proceeds. It is probable, therefore, that these dislocation tangles are either neutral toward, or assist the martensite transformation. Finally, areas of retained martensite are seen in the highly trained alloys, which is consistent with findings in this work and work of other researchers [Ref. 9,10,15]. It is probable that some martensite plates exist in other areas of the specimens in metastable form, and rapidly nucleate and grow as stress is increased or temperature decreased below M_s . This certainly appears to be the case in Figure 21, for example. If this is the case,

that the submicrostructure adjusts itself to accommodate a particular variant of martensite growth, then this certainly helps explain TWSM. The refinement, improvement or increased definition of the substructure with cycling would account for the ability of specimens to exhibit increased TWSM with training.

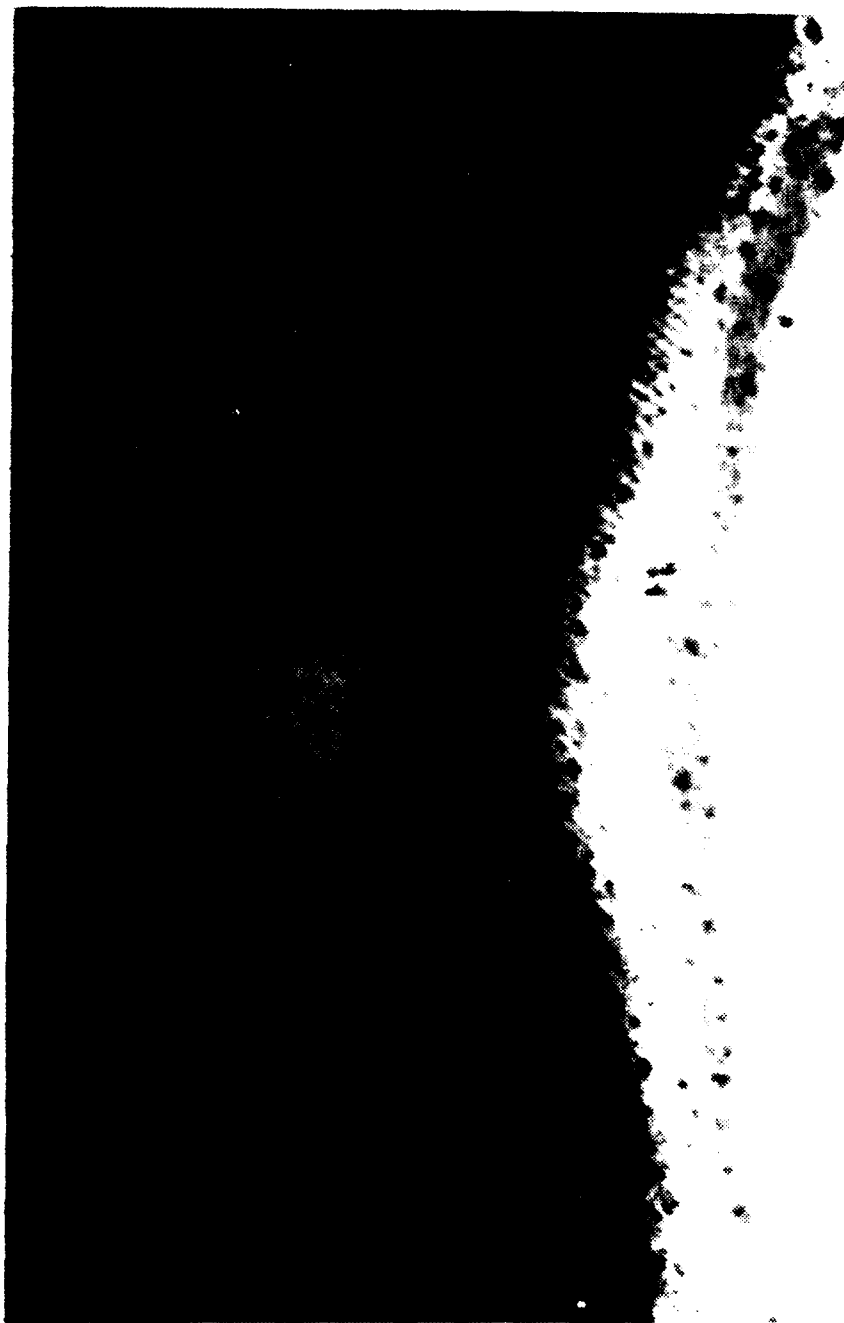


Figure 13. Specimen D-11 (untrained). 23,500X



Figure 14. Specimen D-10 (3 training cycles). Individual lines are dislocations. 39,000X

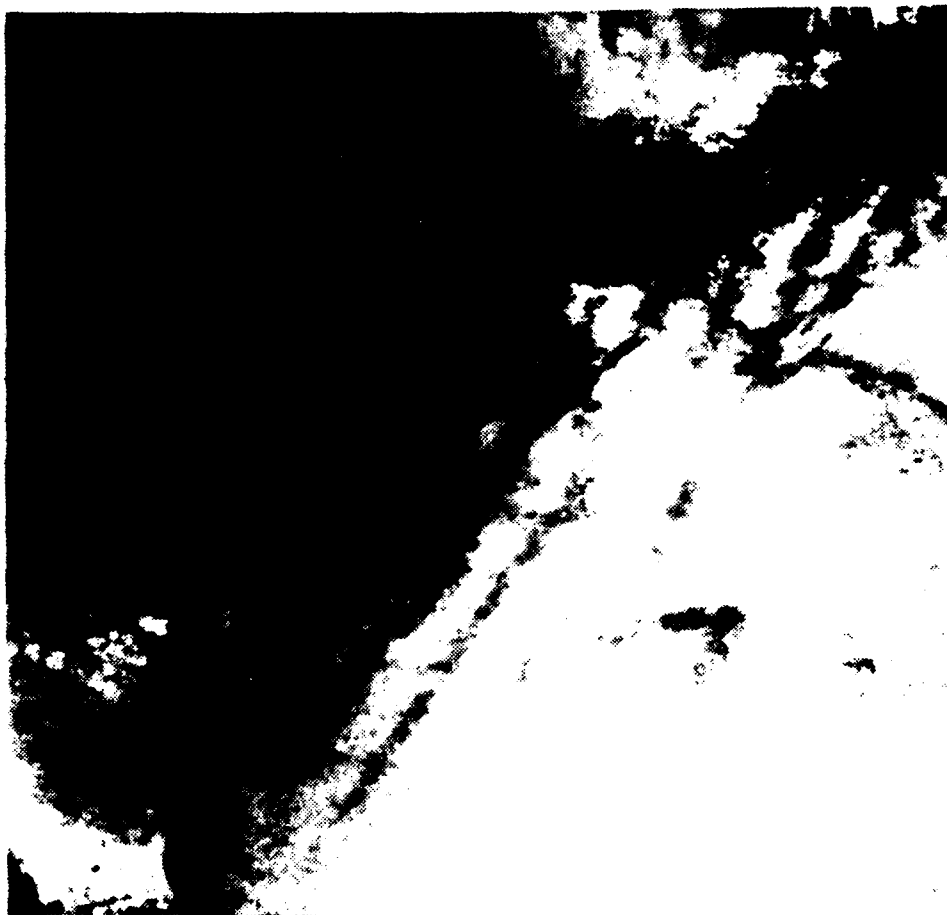


Figure 15. Specimen D-10 (3 training cycles). Light and dark parallel regions are evidenced along with some straight features between uppermost parallel regions. 26,500X



Figure 16. Specimen D-10 (3 training cycles). Same area as Figure 15 at 53,000X.



Figure 17. Specimen D-10 (3 training cycles). 79,500X



Figure 18. Specimen D-5 (5 training cycles). Regions similar to those of specimen D-10 are shown. 26,500X



Figure 19. Specimen D-5 (5 training cycles). Same area as Figure 18. 39,000X

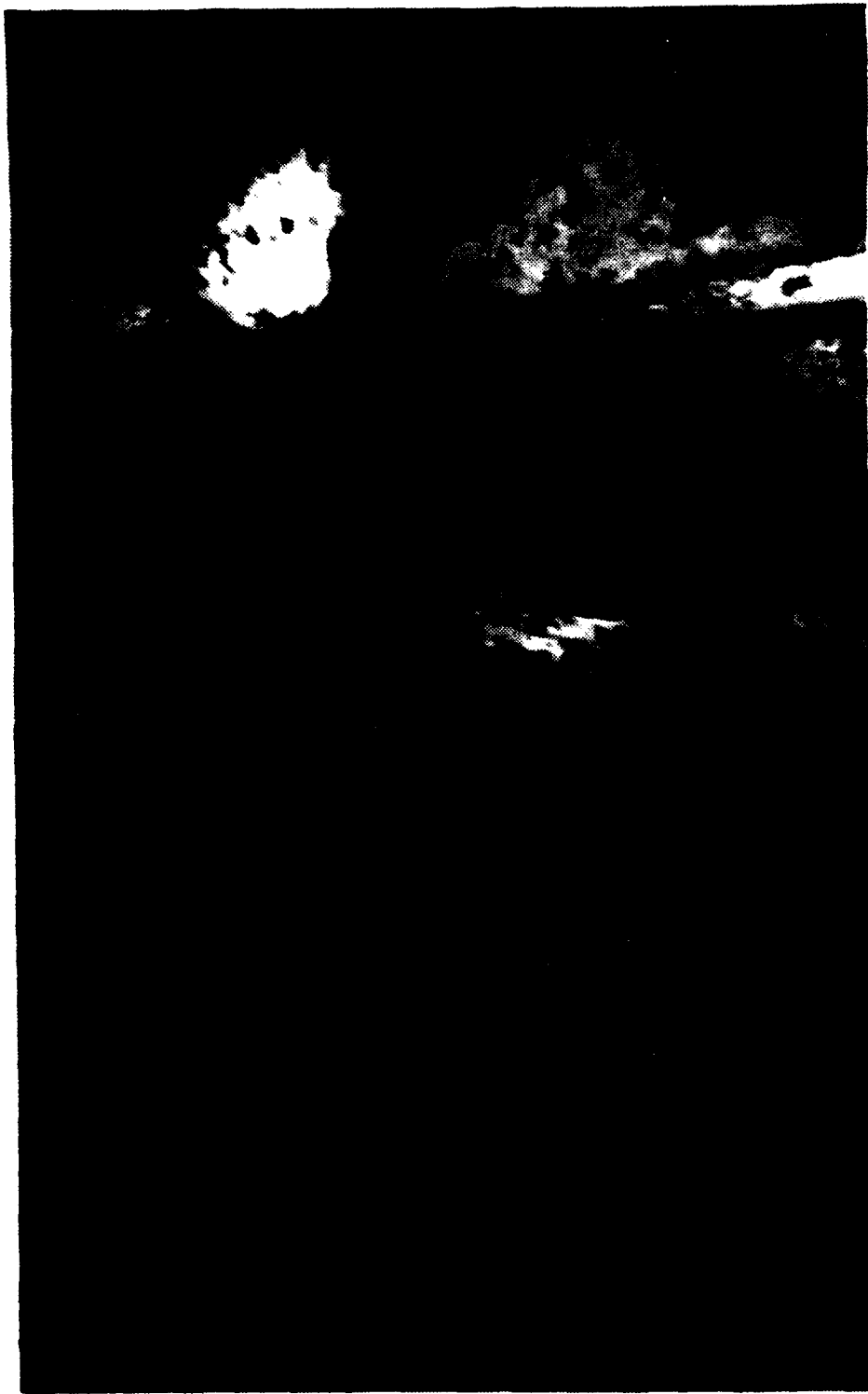


Figure 20. Specimen D-5 (5 training cycles). Preferential polishing has outlined areas where martensite plates existed. There are linear features, possibly dislocations, on the left part of the photo micrograph. 39,000X



Figure 21. Specimen D-4 (15 training cycles). Regions of former martensite plates are shown. A parallel array of dislocations is in the background. Parallel "vestigial" markings under lower plate region is shown. 26,500X



Figure 22. Specimen D-4 (15 training cycles). Same region as Figure 21. 53,000X



Figure 23. Specimen D-4 (15 training cycles). Same region as Figure 21. 79,500X

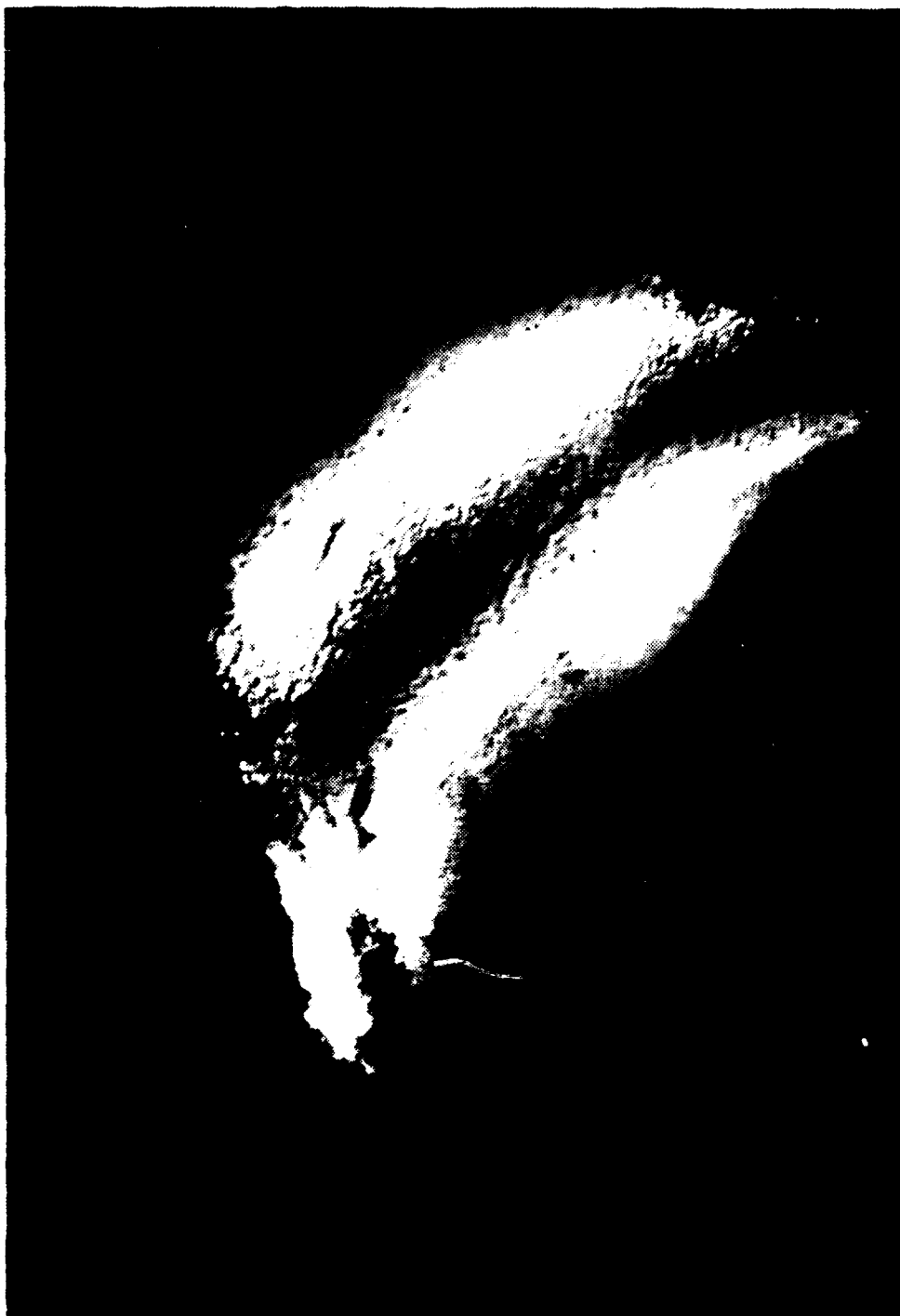


Figure 24. Specimen D-4 (15 training cycles). Area between parallel markings. Dislocations are evident. Two parallel retained martensite plates appear in lower left. 26,500X



Figure 25. Specimen D-6 (20 training cycles). Parallel bands similar to specimen D-10 (3 training cycles) are shown. 26,500X

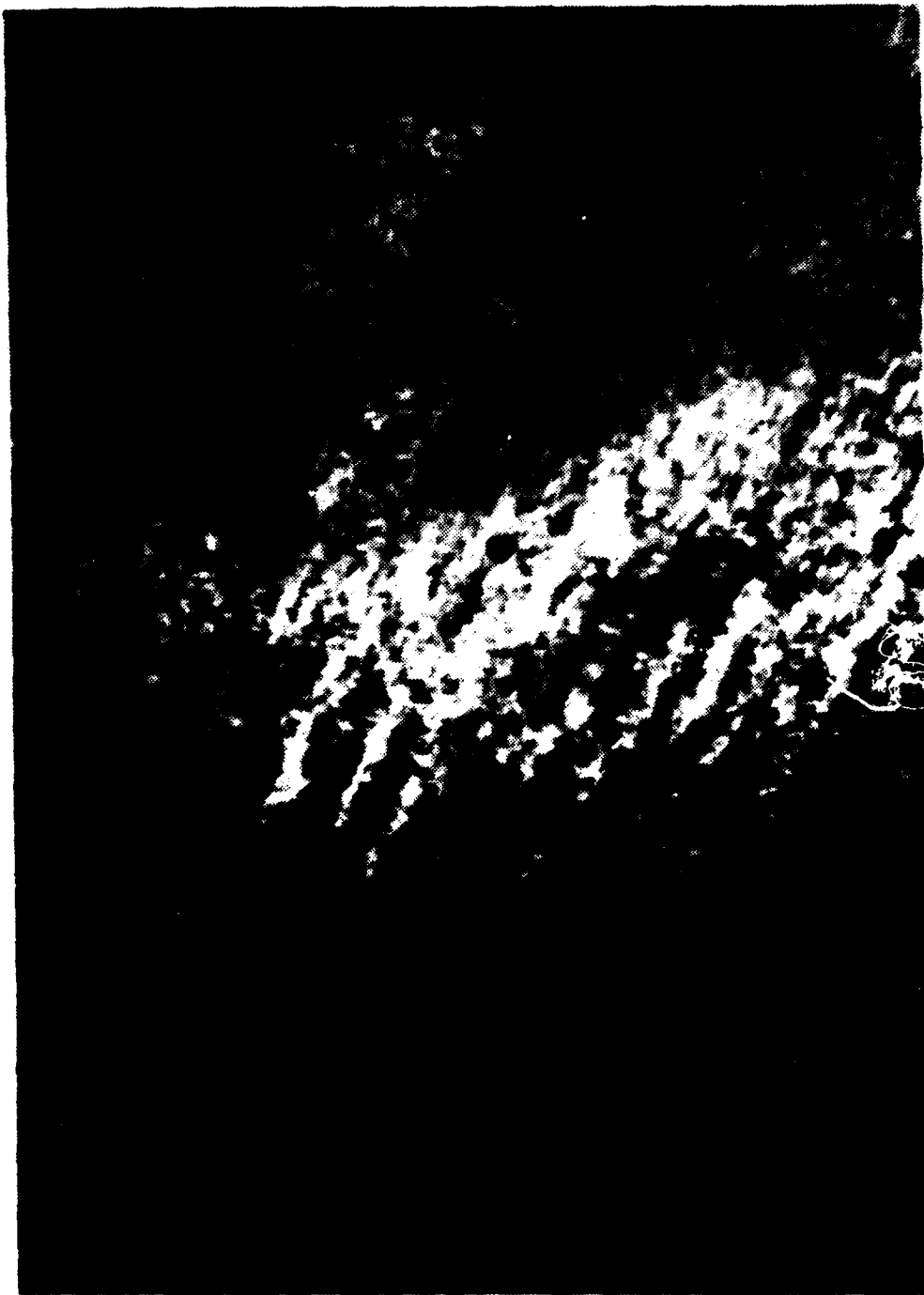


Figure 26. Specimen D-6 (20 training cycles).
Same region as Figure 25 at 53,000X.



Figure 27. Specimen D-7 (30 training cycles). Retained martensite plate with heavily dislocated area surrounding them. 26,500X

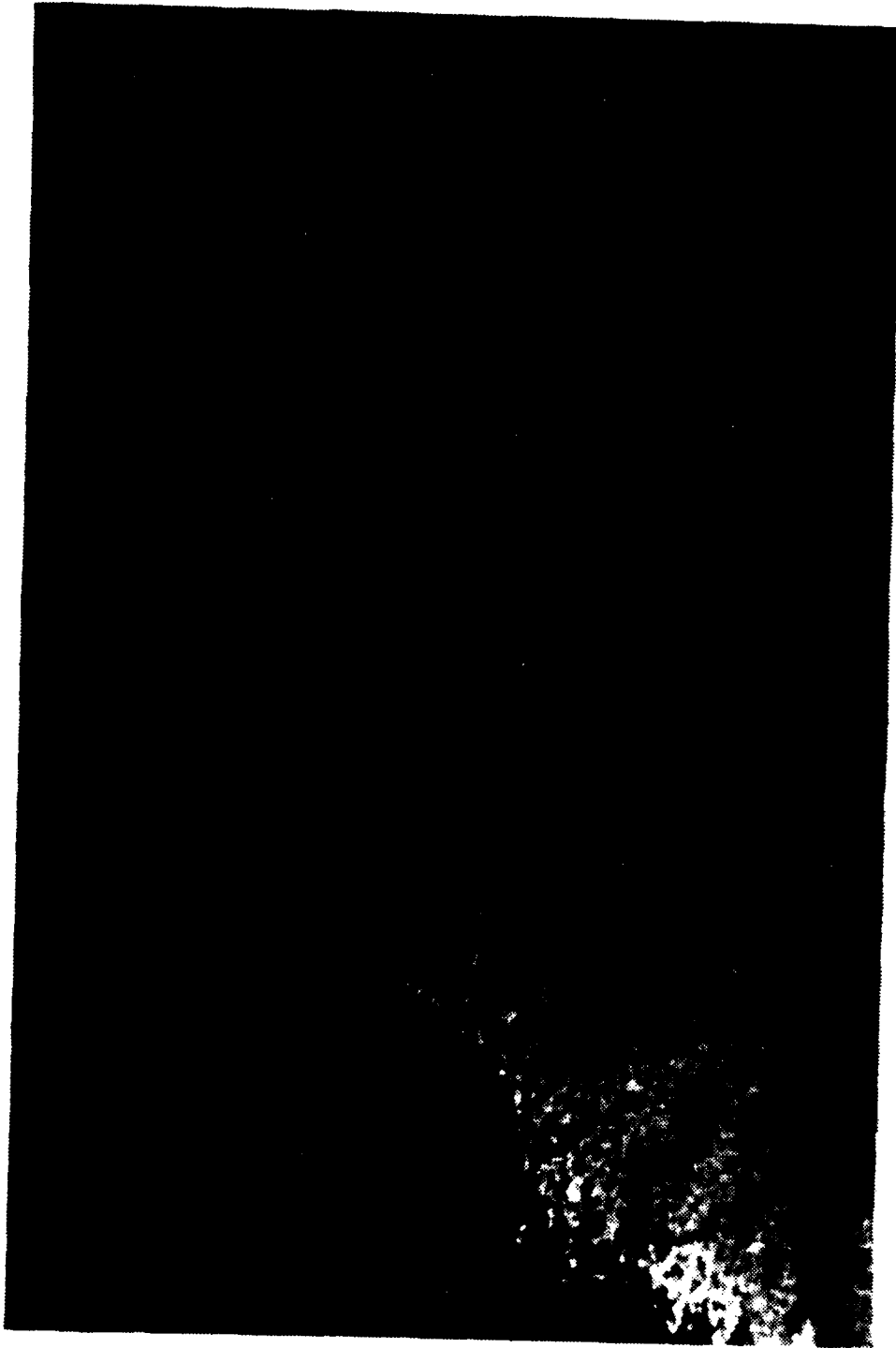


Figure 28. Specimen D-7 (30 training cycles). Martensite plate arrangement with debris adjoining plate area. 39,000X



Figure 29. Specimen D-7 (30 training cycles). 79,500X



Figure 30. Diffraction pattern of area shown in Figure 29.



Figure 31. Specimen D-7 (30 training cycles). Dislocation tangles. 53,000X



Figure 32. Specimen D-7 (30 training cycles). Same area as Figure 31 at 120,000X. Individual dislocations can be seen.

V. CONCLUSIONS

This study has demonstrated that polycrystalline Cu-Zn-Al alloys are capable of improving their TWSM when subjected to a number of prior "training" cycles. It is apparent from the data that one could expect to achieve displacements approaching 40 to 50% of the "trained" displacement during TWSM, provided the specimen was subjected to a sufficient number of prior training cycles. A sufficient number is considered to be approximately fifteen based on the data generated from an admittedly small sample group.

Factors which contribute to the improvement of TWSM are:

1. Plastic Deformation - Based on the decreasing amount of induced displacement (Table II) coupled with TEM evidence of increased dislocation density with cycling, it is apparent that light plastic deformation assists the training process and results in improved TWSM. It is concluded, therefore, the initial plastic deformation in the specimens studied in this work was a useful and necessary prerequisite to TWSM.
2. Retained Martensite - As training progresses the specimens retain some amount of martensite. Dislocations generated during training may inhibit the reversion of martensite to parent β phase. During subsequent cycles, this retained martensite does not have to be induced by stress or temperature and thus the training process becomes easier, as

evidenced by the decreasing trend in peak stress (Table IV). While not verified by this study, it is likely that the retained martensite serves as nucleation points for the thermoelastic martensitic transformation during TWSM.

3. Substructural Refinement - The combination of light plastic deformation and retained martensite leads to subtle substructural changes whose end result is the adjustment of the parent matrix in such a manner as to nucleate and grow a particular and preferential variant of martensite. This substructural adjustment continues and becomes more refined with cycling.

As a practical matter, based on the experimental work conducted and data generated in this research, one can achieve optimum TWSM displacements when the alloy, initially in the parent phase, is subjected to some amount of plastic deformation during the first cycle, followed by approximately fifteen training cycles. These training cycles should encompass displacements 100% greater than the desired TWSM displacement. Of course, alloy selection should be based upon temperature requirements allowing training to be conducted between M_f and P_f .

The ability of Cu-Zn-Al alloys to "train" is of practical significance and will undoubtedly be put to use in future application of these materials.

LIST OF REFERENCES

1. Perkins, J., Thermomechanical Aspects of Shape Memory Alloys, presented at the Summer School on "Materials with Shape Memory," Jablonna, Poland, 29 June to 4 July 1981.
2. Delaey, L., Krishnan, R. V., Tas, H., and Warlimont, H., "Review, Thermoelasticity, Pseudoelasticity and the Memory Effects Associated with Martensitic Transformations," Journal of Material Science, Vol. 9, pp. 1521-1535, 1974.
3. Delaey, L., Thienel, J., "Microstructural Changes During SME Behavior," Shape Memory Effects in Alloys (J. Perkins, editor), Proceedings of the 1975 International Symposium on Shape Memory Effects and Applications, Toronto, Canada, pp. 314-350. Plenum Publishing Co., New York, 1975.
4. Delaey, L., Deruytve, A., Aernoudt, E., and Roos, J.R., Report 78R1, Shape Memory Effect, Superelasticity and Damping in Copper-Zinc-Aluminium Alloys, p. 68, February 1978.
5. Johnson, J. M., Thermomechanical Characteristics of Nitinol, M.S. Thesis, Naval Postgraduate School, Monterey, 1975.
6. Nagasawa, A., Enami, K., Ishino, Y. and Nenno S., "Reversible Shape Memory Effect," Scripta Metallurgia Vol. 8, p. 1055, 1974.
7. Otsuka, K., Shinizu, K., "Stress-induced Martensitic Transformations and Martensite - to Martensite Transformation," Proceedings, International Conference on Solid-Solid Phase Transformations, Pittsburgh, PA, August 10-14, 1981.
8. Perkins, J., Edwards, G. R., Such, C. R., Johnson J. M., and Allen, R. R., "Thermomechanical Characteristics of Alloys Exhibiting Martensitic Thermoelasticity," in Shape Memory Effects in Alloys, J. Perkins, editor, (see Ref. 3), pp. 273-303, New York, 1975.
9. Delaey, L., Van Humbeeck, J., Chandrasekaran, M., Janssen, J., Androde, M., and Mwantha, N., "The Cu-Zn-Al Shape Memory Alloys," to be published. 1981.

10. Muesing, W., Thermal Martensitic Transformation Cycling in Cu-Zn-Al Shape Memory Alloys, M.S. Thesis, Naval Postgraduate School, Monterey, 1982.
11. Schroeder, T. A., and Wayman, C. M., "The Two-Way Shape Memory Effect and Other 'Training'," Scripta Metallurgica, Vol. 11, pp. 225-230, 1977.
12. Delaey, L., Chandrasekaran, M., De Jonge, W., Rapacioli, R., and Deruyttene, A., Annual Report, Incra Project No. 238, Shape Memory Effect and Internal Damping in Copper-Aluminium and Cooper-Zinc Based Alloys, p.20, April 1975.
13. Perkins, J., "Residual Stresses and the Origin of Reversible (Two Way) Shape Memory Effects," Scripta Metallurgica, Vol. 8, pp. 1469-1475, 1974.
14. Delaey, L., Perkins, J., Massalski, T.B., "Review: On the Structure and Microstructure of Quenched Beta-Brass Type Alloys," Journal of Material Science, Vol. 7, pp. 1197-1215, 1972.

INITIAL DISTRIBUTION LIST

	No. Copies
1. Defense Technical Information Center Cameron Station Alexandria, Virginia 22314	2
2. Library, Code 0142 Naval Postgraduate School Monterey, California 93940	2
3. Department Chairman, Code 69 Department of Mechanical Engineering Naval Postgraduate School Monterey, California 93940	2
4. Associate Professor Jeff Perkins, Code 69Ps Department of Mechanical Engineering Naval Postgraduate School Monterey, California 93940	5
5. LCDR Richard O. Sponholz 56-12 142 Street Flushing, New York 11355	1

DATE
ILME